

Annual Review of Marine Science

GEOTRACES: Accelerating Research on the Marine Biogeochemical Cycles of Trace Elements and Their Isotopes

Robert F. Anderson

Lamont-Doherty Earth Observatory, Columbia University, Palisades, New York 10964, USA;
email: boba@ldeo.columbia.edu

Annu. Rev. Mar. Sci. 2020. 12:49–85

First published as a Review in Advance on
July 23, 2019

The *Annual Review of Marine Science* is online at
marine.annualreviews.org

<https://doi.org/10.1146/annurev-marine-010318-095123>

Copyright © 2020 by Annual Reviews.
All rights reserved

Keywords

trace elements, radionuclides, isotopes, ligands, colloids, GEOTRACES

Abstract

The biogeochemical cycles of trace elements and their isotopes (TEIs) constitute an active area of oceanographic research due to their role as essential nutrients for marine organisms and their use as tracers of oceanographic processes. Selected TEIs also provide diagnostic information about the physical, geological, and chemical processes that supply or remove solutes in the ocean. Many of these same TEIs provide information about ocean conditions in the past, as their imprint on marine sediments can be interpreted to reflect changes in ocean circulation, biological productivity, the ocean carbon cycle, and more. Other TEIs have been introduced as the result of human activities and are considered contaminants. The development and implementation of contamination-free methods for collecting and analyzing samples for TEIs revolutionized marine chemistry, revealing trace element distributions with oceanographically consistent features and new insights about the processes regulating them. Despite these advances, the volume and geographic coverage of high-quality TEI data by the end of the twentieth century were insufficient to constrain their global biogeochemical cycles. To accelerate progress in this field of research, marine geochemists developed a coordinated international effort to systematically study the marine biogeochemical cycles of TEIs—the GEOTRACES program. Following a decade of planning and implementation, GEOTRACES launched its main field effort in 2010. This review, roughly midway through the field program, summarizes the steps involved in designing the program, its management structure, and selected findings.

ANNUAL
REVIEWS **CONNECT**

www.annualreviews.org

- Download figures
- Navigate cited references
- Keyword search
- Explore related articles
- Share via email or social media

1. INTRODUCTION

The biogeochemical cycles of trace elements and their isotopes (TEIs) are an active area of oceanographic research due to their role in biological activity and their use as tracers of oceanographic processes. Many trace elements are essential for life, including Fe, Zn, Co, Cu, Mn, Ni, and Cd. Often referred to as micronutrients, they serve as cofactors in enzymes engaged in the cellular transformation and assimilation of C, N, and P, including photosynthesis and respiration (e.g., Lohan & Tagliabue 2018, Morel & Price 2003, Sunda 2012, Twining & Baines 2013). A scarcity of these elements limits the overall productivity of marine ecosystems (e.g., Boyd et al. 2007, Browning et al. 2017, Moore 2016, Moore et al. 2013, Saito et al. 2005, Tagliabue et al. 2017) and the ecosystem capacity for N fixation (Moore et al. 2009) while also influencing the taxonomic composition of communities (Boyd et al. 2017, Hutchins & Boyd 2016, Moore et al. 2013, Sunda 2012, Twining & Baines 2013).

TEIs also provide diagnostic information about the physical, geological, and chemical processes that supply or remove solutes in the ocean (e.g., Anderson et al. 2016; Geibert 2018; Hayes et al. 2015b, 2018a; Jeandel 2016; Jeandel & Vance 2018; Sanial et al. 2018). Many of these same TEIs provide information about ocean conditions in the past, as their imprint on marine sediments can be interpreted to reflect changes in ocean circulation, biological productivity, the ocean carbon cycle, and more (e.g., Chase et al. 2018, Henderson 2002). Other TEIs have been introduced as the result of human activities and are considered contaminants, such as Pb and Hg (e.g., Boyle et al. 2014, Lamborg et al. 2014). In addition to these sources, the anticipated growth of seabed mineral extraction may alter future trace element distributions in the deep sea (Lusty & Murton 2018).

2. THE ORIGIN AND EVOLUTION OF RESEARCH ON MARINE TRACE ELEMENTS

Prior to the mid-1970s, analysis of seawater for trace elements was often compromised by contamination (Boyle & Edmond 1975; Boyle et al. 1976; Bruland 1983; Bruland et al. 1978a, 1979). The development and implementation of contamination-free methods revolutionized marine chemistry, revealing trace element distributions with oceanographically consistent features (Boyle et al. 1976) and new insights about the processes regulating them (Bruland 1983). Despite these advances, the volume and geographic coverage of high-quality TEI data by the end of the twentieth century were insufficient to constrain their global biogeochemical cycles (Boyd & Ellwood 2010). A compilation in 2004, a quarter century after the trace element revolution, found only 25 profiles worldwide of dissolved Fe (dFe) measured to 2,000-m depth (**Supplemental Figure 1**), due in large part to the labor-intensive nature of contamination-free sampling. For example, collecting the samples for the concentration profiles of Zn, Cu, Ni, and Cd reported by Bruland (1980) required up to six days for each station (K.W. Bruland, personal communication). The global coverage required to study biogeochemical cycles was simply not possible using this technology. A new plan was needed to accelerate TEI research.

Inspired by the Geochemical Ocean Sections Study (GEOSECS) program of the 1970s (Craig & Turekian 1980), which provided the first systematic survey of ocean chemistry at a global scale (e.g., Broecker & Peng 1982) and revolutionized our understanding of marine biogeochemical cycles of C and major nutrients, marine geochemists sought to develop an analogous study for TEIs. With support from the US National Science Foundation, the Centre National de la Recherche Scientifique, and the Université Paul Sabatier, an international planning workshop held in Toulouse, France, in April 2003 established the principal research questions and hypotheses that would serve as the foundation for a new program, to be called GEOTRACES.

Supplemental Material >

A planning committee, established in 2004 with support from the Scientific Committee on Oceanic Research (SCOR), prepared a science plan for GEOTRACES that defined the program's mission: "to identify processes and quantify fluxes that control the distributions of key trace elements and isotopes in the ocean, and to establish the sensitivity of these distributions to changing environmental conditions" (GEOTRACES Plan. Group 2006, p. 1). The priorities set by this plan are expected to guide GEOTRACES through the end of the program, anticipated to occur in the mid-2020s.

Data on Fe from the Atlantic and Pacific collected during the first decade of GEOTRACES fieldwork (**Figure 1**) illustrate the degree to which TEI research has accelerated. Comparing the state of the art in 2004 (25 profiles of dFe to a depth of at least 2,000 m, as described above, and even less for other TEIs) with the results from less than a decade of GEOTRACES research leads to the questions "How did this come about?" and "What was learned?" This review aims to provide answers.

3. GUIDING PRINCIPLES AND IMPLEMENTATION STRATEGY

Drawing on the experience of previous oceanographic programs, including GEOSECS, the World Ocean Circulation Experiment (WOCE), and the Joint Global Ocean Flux Study (JGOFS), the following guidelines preceded formulation of detailed plans: (a) Define the mission, hypotheses, questions, and related goals first, creating a target to guide further planning activities; (b) design a manageable strategy to meet achievable goals; (c) stay focused on the mission and avoid temptations that would lead to mission creep; and (d) conclude the program when the mission has been completed. Within the context of these guidelines, the planning committee further adopted three principles for the science plan: (a) The scope should be global; (b) planning should encompass concurrent investigation of multiple TEIs; and (c) to meet these first two principles, the program must involve international participation, as no single nation has the resources to complete such a study alone.

A decade of planning and implementation prepared the launch of the main GEOTRACES field program in 2010. A study of global scope and involving several nations required extensive planning and coordination to optimize resources and ensure adequate ocean coverage. The production of TEI data by multiple labs employing novel methods for challenging measurements necessitated rigorous quality control to ensure internal consistency across results. The management of diverse types of data depended on a sophisticated data management system to collect, organize, and distribute the data. Only an appropriate level of centralized oversight could ensure the seamless integration of these activities, and the creation of a single communication hub facilitated coordination. The **Supplemental Material** provides details concerning the planning meetings to establish research priorities, the standing committees to oversee data quality and data management, the Scientific Steering Committee to oversee all activities of the program, the International Project Office to support each of these activities, and oversight of the entire process by SCOR.

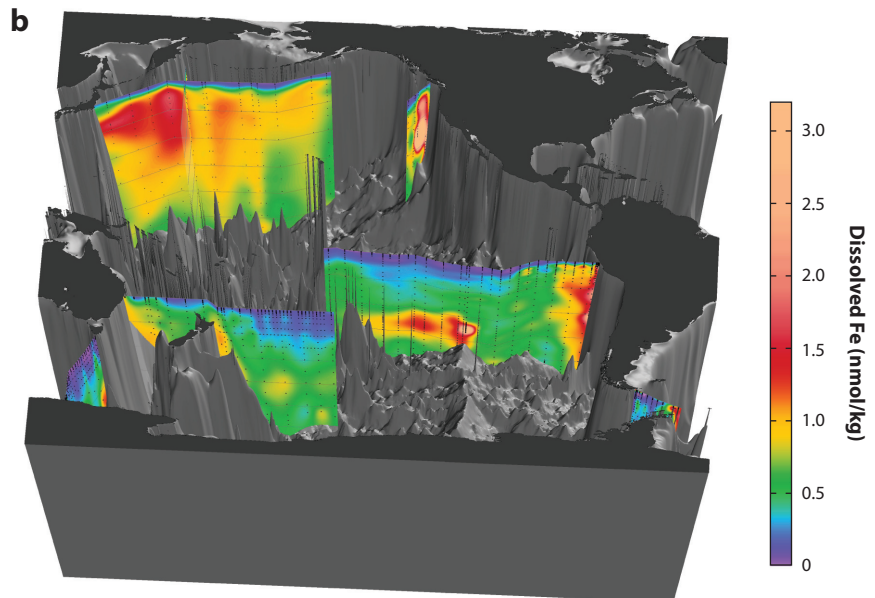
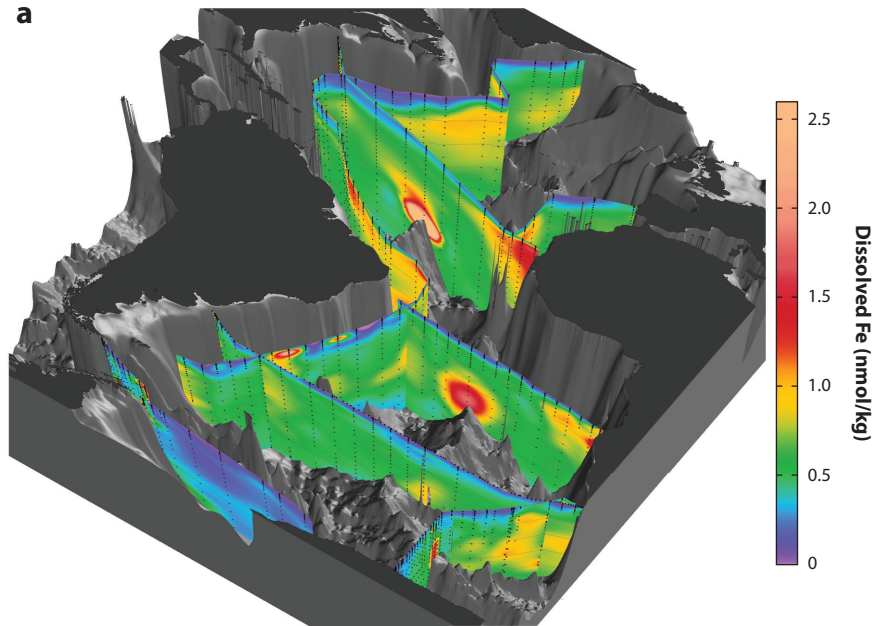
Supplemental Material >

4. ACCOMPLISHMENTS

This review of GEOTRACES findings begins with an illustration of the contrasting distributions of three essential micronutrients (Fe, Zn, and Co; **Figure 2**) in the Atlantic, comparing their distributions with those of the macronutrient phosphate and the lithogenic element Al. This introduction is followed by an overview of GEOTRACES activities related to the three guiding themes of the program: (a) fluxes and processes at ocean interfaces (Section 4.1), (b) internal

cycling of TEIs (Section 4.2), and (c) the development of proxies for past change (Section 4.3). The review concludes with a view of the future and how programs yet to be created can build on the GEOTRACES legacy (Section 5).

The distributions of major nutrients (N, P, and Si) in the ocean reflect biological consumption in surface waters, regeneration at depth, and redistribution by ocean circulation. These processes



(Caption appears on following page)

Figure 1 (Figure appears on preceding page)

Dissolved Fe concentrations in (a) the Atlantic and (b) the Pacific, extracted from rotating three-dimensional animations available in the eGEOTRACES electronic atlas (<http://www.egeotraces.org>). Elevated concentrations of dissolved Fe are present around the crest of mid-ocean ridges, indicating hydrothermal sources, and near continental margins, indicating sources from sediments and dust. Data for panel a are originally from Eric Achterberg, Andrew Bowie, Ken Bruland, Fanny Chever, Tim Conway, Hein de Baar, Seth John, Maarten Klunder, Patrick Laan, Francois Lacan, Rob Middag, Abigail Noble, Micha Rijkenberg, Mark Saito, Geraldine Sarthou, Christian Schlosser, Peter Sedwick, and Jinfeng Wu; data for panel b are originally from Andrew Bowie, Philip Boyd, Kenneth Bruland, Michael Ellwood, Hein de Baar, Josh Helgoe, Seth John, Maarten Klunder, Tomoharu Minami, Jun Nishioka, Hajome Obata, Tomas Remenyi, Saeed Roshan, Peter Sedwick, Yoshiki Sohrin, Bettina Sohst, Charles-Edouard Thuroczy, Claire Till, Ashley Townsend, Emily Townsend, Pier van der Merwe, Jinfeng Wu, Kathrin Wuttig, and Linjie Zhengg. Data are available in the GEOTRACES Intermediate Data Product 2017 (Schlitzer et al. 2018). Graphics were created by Reiner Schlitzer.

are evident in the distribution of phosphate along a meridional transect from Iceland to Antarctica generated by splicing multiple GEOTRACES sections (inset map in **Figure 2**; **Supplemental Figure 3** shows a global map of GEOTRACES sections). Phosphate is depleted in low-latitude surface waters (**Figure 2a**), reflecting biological consumption, and enriched in deep waters entering the Atlantic from the south, recording the long history of regenerated nutrients accumulating in these old water masses. North Atlantic Deep Water, which contains a large component of nutrient-depleted surface water, has intermediate phosphate concentrations.

Of the three micronutrients discussed here, Zn has the longest residence time in the ocean; its residence time is longer than the timescale for ocean mixing (Roshan et al. 2016), so its distribution follows that of phosphate most closely (**Figure 2b**). However, Zn is removed more efficiently than P from surface waters of the Southern Ocean (Section 4.2.2), causing Zn depletion in water masses formed from Antarctic surface waters (Subantarctic Mode Water and Antarctic Intermediate Water). The residence time of Co is less than the mixing time of the ocean (Hawco et al. 2018, Tagliabue et al. 2018), so its distribution is influenced more strongly by its sources than the distribution of Zn is. Mobilization from shelf and upper-slope sediments (Section 4.2.2) produces the maximum in dCo at intermediate depths (**Figure 2c**). The residence time of dFe is not well constrained, but synthesis of GEOTRACES findings suggests no more than a few decades in the deep sea (Hayes et al. 2018a). Consequently, the distribution of dFe is patchy (**Figure 2d**), dominated by its local sources (Section 4.1).

The distribution of dAl (**Figure 2e**), a major crustal element without known biological function, clearly differs from those of the nutrients. Elevated concentrations reflect North Atlantic sources, including Saharan dust (evident in the upper water column of the subtropics), and mobilization from subpolar sediments. The residence time of dAl in the deep sea is sufficiently long that the sedimentary source is still imprinted on North Atlantic Deep Water as it enters the Southern Ocean (**Figure 2e**).

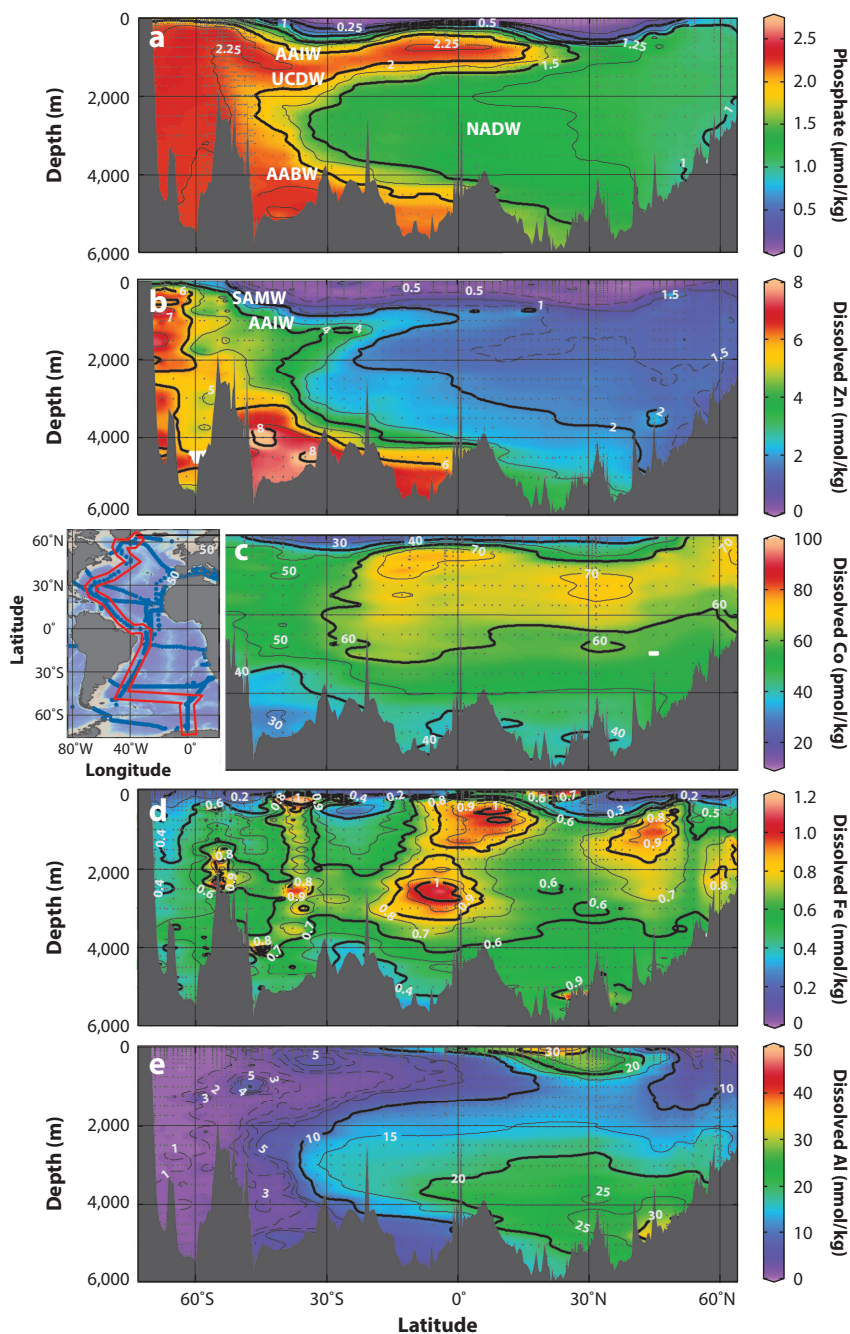
The processes described above and their impact on TEI distributions are discussed in greater detail in the sections that follow.

4.1. Theme 1: Fluxes and Processes at Ocean Interfaces

This section describes results from GEOTRACES studies of ocean interfaces following the framework illustrated in **Figure 3**. Section 4.2 takes a similar approach when describing the cycling of TEIs within the ocean.

4.1.1. Aerosols. Because the deposition of aerosols represents an important source of certain TEIs in remote areas of the ocean (Jickells & Moore 2015, Jickells et al. 2005), many

GEOTRACES cruises have determined aerosol abundance and composition. Back-trajectory analyses tie the aerosols at their point of sampling back to their sources, while normalization to major lithogenic elements allows the contributions of natural and anthropogenic trace elements to be distinguished (Buck et al. 2019; Jickells et al. 2016; Shelley et al. 2015, 2017, 2018). In addition



(Caption appears on following page)

Figure 2 (Figure appears on preceding page)

Meridional sections down the length of the Atlantic created by splicing data from multiple GEOTRACES sections (*inset map*). (a) Phosphate concentrations [from the GEOTRACES Intermediate Data Product 2017 (Schlitzer et al. 2018)]. (b) Dissolved Zn concentrations (Middag et al. 2019; P. Croot, unpublished data). (c) Dissolved Co concentrations (Dulaquais et al. 2014a,b; M. Boye, unpublished data). (d) Dissolved Fe concentrations (Klunder et al. 2011, Rijkenberg et al. 2014). (e) Dissolved Al concentrations (Middag et al. 2011, 2015; P. Croot, unpublished data). All data, including otherwise unpublished data, are available in the GEOTRACES Intermediate Data Product 2017 (Schlitzer et al. 2018). Figure produced using Ocean Data View (<http://odv.awi.de>). Abbreviations: AABW, Antarctic Bottom Water; AAIW, Antarctic Intermediate Water; NADW, North Atlantic Deep Water; SAMW, Subantarctic Mode Water; UCDW, Upper Circumpolar Deep Water.

to the Atlantic, where aerosol sampling has been underway for several years (see references above), GEOTRACES is beginning to fill in the historically undersampled Pacific. Although aerosols represent a minor contribution of most TEIs in the eastern tropical South Pacific (Buck et al. 2019), they serve as a significant source of Fe to the western portion of the South Pacific subtropical gyre (Ellwood et al. 2018).

The impact of aerosols on ocean chemistry and biology depends on the solubility of TEIs in aerosols as well as on aerosol abundance and composition. Building on earlier studies (e.g., as summarized in Sholkovitz et al. 2012), GEOTRACES investigators have assessed aerosol solubility and the many factors controlling it (Aguilar-Islas et al. 2010; Fishwick et al. 2014, 2018; Shelley et al. 2018), including their abundance, source, and size fraction (Jickells et al. 2016, Shelley et al. 2018); the organic compounds in aerosols that enhance TEI solubility (Wozniak et al. 2013, 2014, 2015); and the presence of metal-binding ligands in seawater (Fishwick et al. 2014, 2018).

New approaches to evaluate aerosol fluxes to the ocean based on the mass budgets of naturally occurring radionuclides, including ^7Be (Kadko et al. 2015) and long-lived Th isotopes (Hayes et al. 2013, Hsieh et al. 2011), are under development in GEOTRACES. These new approaches are compared against one another, against fluxes calculated using traditional settling velocities,

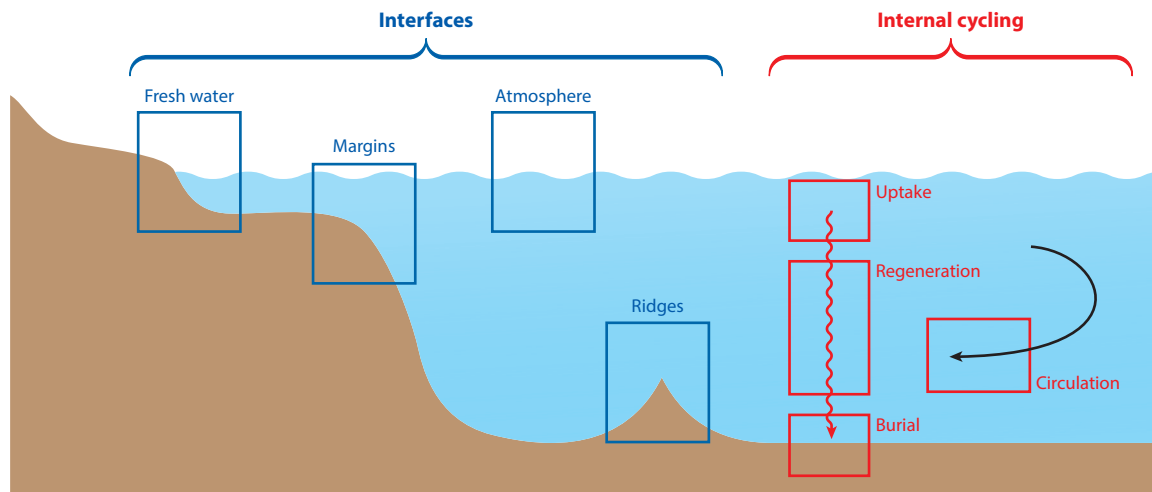


Figure 3

The main targets for investigation pertaining to two of the three main research themes in GEOTRACES: sources and sinks of trace elements and their isotopes at ocean interfaces (theme 1) and cycling of trace elements and their isotopes within the ocean (theme 2). Developing this conceptual framework at the beginning of GEOTRACES has aided in setting priorities throughout the program. Figure adapted from the GEOTRACES science plan (GEOTRACES Plan. Group 2006).

and against mean annual fluxes estimated using models (Anderson et al. 2016, Baker et al. 2016, Shelley et al. 2017).

Among the micronutrients, the distribution of Fe is the most affected by aerosol deposition. Elevated concentrations of dFe in surface waters correlate with concentrations of dAl across broad expanses of the Atlantic (Hatta et al. 2015, Rijkenberg et al. 2014), consistent with previous studies that used Al as a tracer of dust (Measures et al. 2008, Moore et al. 2009). The residence times of other micronutrients are sufficiently long that dust is not thought to serve as a significant source. Co, for which the evidence is contradictory, may be an exception (Dulaquais et al. 2014a; Noble et al. 2012, 2017). The first biogeochemical model for Co suggests that dust is a minor, though nonnegligible, source of Co in the North Atlantic (Tagliabue et al. 2018).

4.1.2. Rivers. Despite the general loss of the operationally defined dFe load carried by rivers through coagulation and sedimentation in estuaries (Boyle et al. 1977), elevated concentrations of dFe were observed in the low-salinity waters of the Amazon plume over a distance of more than 1,000 km from the mouth (Rijkenberg et al. 2014). Similarly, levels of dCo were higher in the Amazon plume (Dulaquais et al. 2014a). Farther north in the Atlantic, Noble et al. (2017) also found a negative correlation between dCo and salinity, indicating a source from rivers and/or groundwater.

In contrast to dFe, which is largely removed in estuaries, desorption from particles mobilizes excess Ba, Cu, and Ni in the Ganges–Brahmaputra estuarine system, supplying to the northern Indian Ocean approximately three times as much Ba (Samanta & Dalai 2016, Singh et al. 2013) and between twice as much and an order of magnitude more dCu and dNi compared with the dissolved load (Samanta & Dalai 2018). Operationally defined dissolved rare earth elements undergo a more complex process: Those occurring mainly as colloids are removed at low salinity within the Amazon estuarine mixing zone (similar to the situation for Fe), while particulate rare earth elements, potentially including previously coagulated colloids, are subsequently remobilized at greater salinity in the outer estuary (Rousseau et al. 2015). Similar processes were detected in the northern Bay of Bengal, where inverse modeling identified a source of dissolved rare earth elements thought to reflect mobilization from particles delivered by the Ganges–Brahmaputra system (Singh et al. 2012).

4.1.3. Sources and sinks at ocean margins. An unexpected finding among GEOTRACES observations is the widespread presence of plumes of elevated dFe concentrations spreading seaward from continental slopes (**Figure 1**). For example, Fe mobilized in the Sea of Okhotsk and around the Kurile Islands has been traced thousands of kilometers east into the subarctic North Pacific, where it serves as an important source for the ecosystem (Nishioka & Obata 2017).

Fe isotopes have been invaluable for discriminating among different sources of Fe in the ocean, including the dFe in margin-related plumes. Mobilization by nonreductive dissolution of lithogenic Fe is evident in the heavy $\delta^{56}\text{Fe}$ of dFe along the western margin of the North Atlantic (Conway & John 2014b), in the deep Cape Basin (Abadie et al. 2017), and in the western tropical Pacific (Labatut et al. 2014). Conway & John (2014b) interpreted the $\delta^{56}\text{Fe}$ of dFe (**Figure 4d**) along a zonal transect across the subtropical North Atlantic to indicate a dust origin for 71–87% of the deep-water dFe, including the deep Fe plume spreading seaward from the margin of Africa (**Figure 4b**), located under the plume of Saharan dust. An eastward decrease in $\delta^{56}\text{Fe}$ within that plume was thought to reflect a smaller source of dFe mobilized reductively from African margin sediments. The much lighter $\delta^{56}\text{Fe}$ signature (**Figure 4c**) of the deep dFe plume spreading from the Peru margin (**Figure 4a**) suggests a much greater contribution there than off Africa from reductive mobilization in sediments, where the signal can be traced as much as 4,000 km to the west.

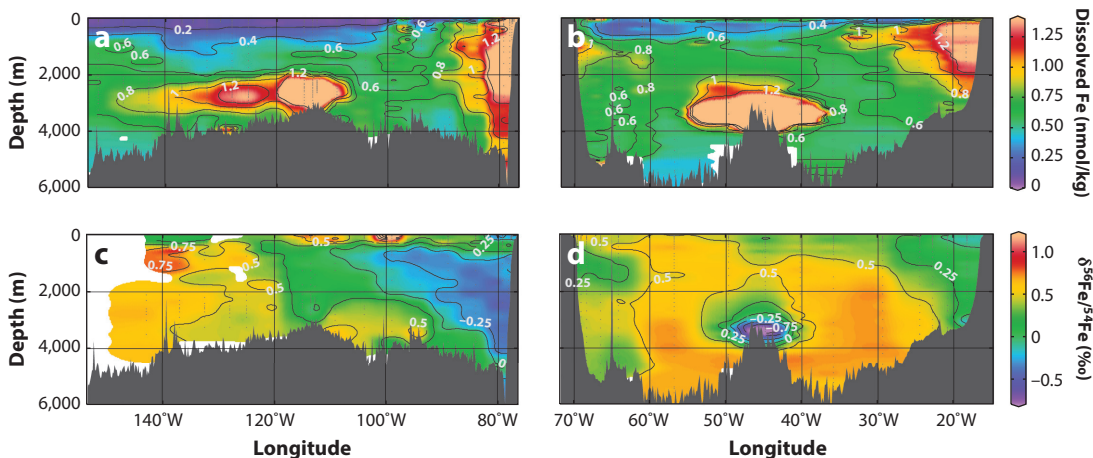


Figure 4

(*a,b*) Concentrations and (*c,d*) isotopic compositions of dissolved Fe along zonal GEOTRACES sections between Peru and Tahiti (*left panels*) and between North America and North Africa (*right panels*). Elevated Fe concentrations are seen in plumes emanating from midocean ridges and off eastern boundary margins. The lighter Fe isotope signature near the margins reflects an Fe source from reductive mobilization of Fe in sediments. Data are from Conway & John (2014b), Fitzsimmons et al. (2017), Hatta et al. (2015), John et al. (2018), Resing et al. (2015), and unpublished results from K. Bruland, P. Sedwick & J. Wu available in the GEOTRACES Intermediate Data Product 2017 (Schlitzer et al. 2018). Figure produced using Ocean Data View (<http://odv.awi.de>).

None of the 13 ocean models examined in an Fe model intercomparison project (Tagliabue et al. 2016) reproduced the plume observed at depths of 1–3 km off Peru (John et al. 2018), so processes absent in the models must be responsible for the plume. John et al. (2018) concluded that downward transport by reversible scavenging of dFe initially mobilized from shelf and upper-slope sediments was most likely to contribute to the deep Fe plume.

Sanial et al. (2018) coupled the distributions of ^{228}Ra and dFe off the Peru margin and estimated that the Fe flux (per unit area) from shelf sediments is approximately three times the flux from slope sediments, consistent with the origin of the deep dFe plume suggested by John et al. (2018). However, they also noted that little of the Fe mobilized on the shelf survives beyond the shelf break. Off-shelf transport of Fe was similarly limited during a GEOTRACES process study in the northeast Atlantic (Birchill et al. 2019). The extent to which Fe mobilized on shelves is trapped there and the processes that generate the observed Fe plumes spreading offshore from continental slopes are suitable topics for future process studies.

Continental margins represent an important source of Co (Figure 5). Unlike Fe, the greatest dCo concentrations occur at depths corresponding to the shelf and upper slope (compare the distributions of dCo in Figure 5*a,b* with those of dFe in Figure 4*a,b*). Co is associated with Mn oxides, and the greater flux of organic matter to shelf and upper-slope sediments is expected to generate more reducing conditions there than at greater water depths, mobilizing Mn as well as the Co associated with it (Hawco et al. 2016, Noble et al. 2017).

Rivers and margin sediments are thought to be the principal sources of Co to the ocean (Dulaquais et al. 2014a; Hawco et al. 2016, 2018; Noble et al. 2017, Tagliabue et al. 2018), while dust appears to be significant only locally (Section 4.1.1). However, the inferred contributions of each of these sources to the overall supply of Co to the ocean vary substantially among these studies. Further investigation will improve estimates of Co supply.

Sources of TEIs have been traced using the imprint left on the isotopic composition (ϵ_{Nd}) of dNd (e.g., Jeandel 2016). Behrens et al. (2018) used ϵ_{Nd} to follow TEI input from continental

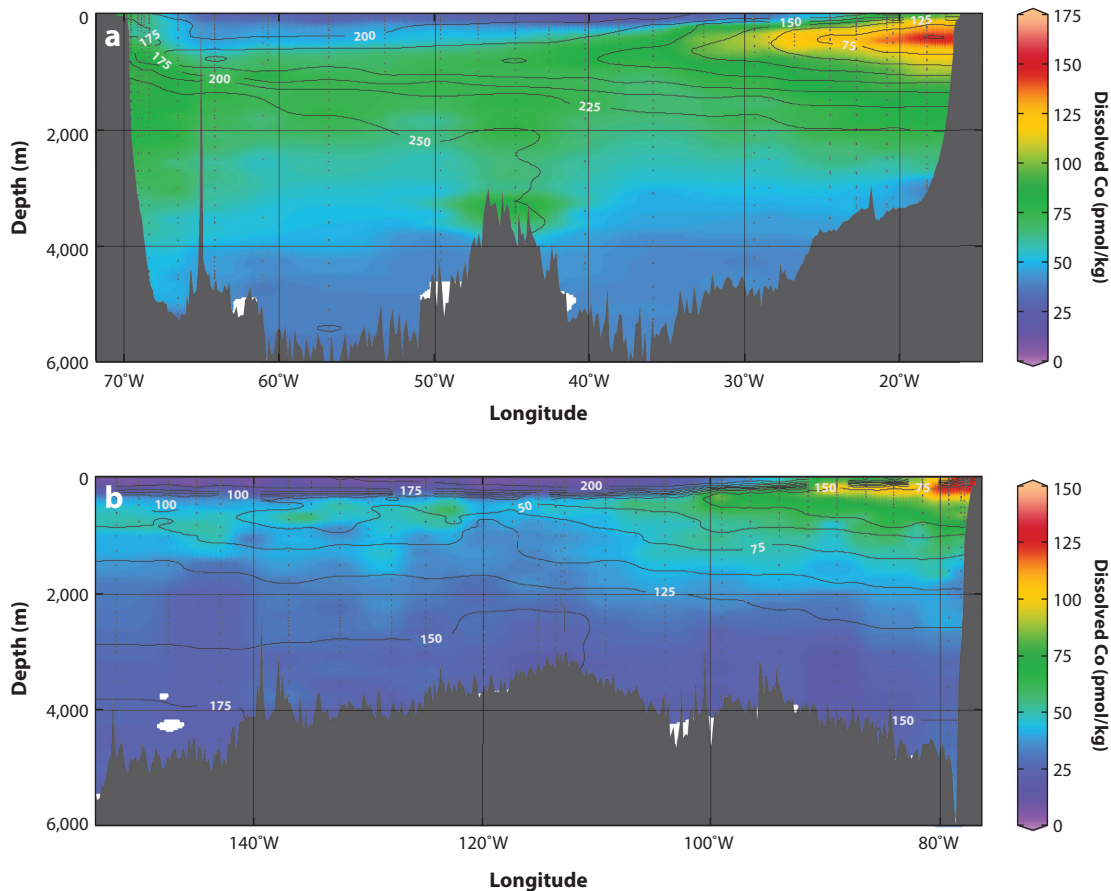


Figure 5

Concentrations of dissolved Co measured along zonal GEOTRACES sections (a) between North America and North Africa (Noble et al. 2017) and (b) between Peru and Tahiti (Hawco et al. 2016). Dissolved oxygen concentrations (in $\mu\text{mol/kg}$) are overlain as contours. Elevated Co concentrations are seen within low-oxygen water on the eastern boundary of each section and are thought to reflect the mobilization of Co bound to Mn oxides that are reduced in organic-rich upper-margin sediments, and within Labrador Sea Water roughly between depths of 1,000 m and 2,000 m on the western boundary in panel a. Data are from the GEOTRACES Intermediate Data Product 2017 (Schlitzer et al. 2018). Figure produced using Ocean Data View (<http://odv.awi.de>).

sources with contrasting lithology and age along the western Pacific margin. Measurements of ϵ_{Nd} and $d\text{Nd}$ during repeat occupations of the Panama Basin suggest a substantial source of TEIs from reactive volcanic arc sediments (Grasse et al. 2017). A study of Nd isotopes off the coast of South Africa revealed active boundary exchange in that region as well (Garcia-Solsona et al. 2014).

Continental margins represent both sources and sinks for TEIs, especially for reactive species that are rapidly adsorbed onto sinking particles. Results from early studies of ^{210}Pb (Bacon et al. 1976) as well as ^{230}Th and ^{231}Pa (Anderson et al. 1983) were interpreted to reflect enhanced scavenging and removal from ocean margin systems, where the abundance and flux of particles is elevated by a combination of biological productivity and supply of lithogenic particles eroded from nearby continents. With the higher-quality data available from GEOTRACES, this boundary scavenging effect was confirmed by a study of ^{230}Th and ^{231}Pa along a zonal transect west of Mauritania (Hayes et al. 2015a). Elevated particle concentrations off northwest Africa as a

consequence of high biological productivity and proximity to the source of Saharan dust (Lam et al. 2015) are responsible for the enhanced scavenging and removal of TEIs there.

4.1.4. Hydrothermal systems. The spatial extent of plumes emanating from hydrothermal vents at midocean ridges is another surprising outcome of the GEOTRACES program (German et al. 2016) (**Figures 1** and **4a**). Previous studies had suggested that metals emitted from hydrothermal vents undergo rapid precipitation and sedimentation in close proximity to the vent system (German et al. 1991), but GEOTRACES sections have sampled hydrothermal plumes extending as far as 4,000 km from the ridge source (**Figure 4a**).

In addition to Fe (**Figures 1** and **4**), hydrothermal systems are also sources of Mn (Hatta et al. 2015, Resing et al. 2015), Al (Measures et al. 2015, Resing et al. 2015), Hg (Bowman et al. 2015, 2016), Co (Noble et al. 2017), and Zn (Roshan et al. 2016) and may represent major contributions to TEI cycles. For example, after normalizing excess Zn (i.e., in excess of the amount expected based on the global relationship between Zn and Si) to ^3He and extrapolating globally, Roshan et al. (2016) concluded that hydrothermal systems represent the largest source of dZn to the ocean, lowering the residence time for Zn in the ocean from previous estimates of 11,000–50,000 years to approximately 3,000 years.

Removal in hydrothermal plumes is indicated by the distributions of Pb (Noble et al. 2015), Cu (Jacquot & Moffett 2015), Cd (Conway & John 2015), and rare earth elements (Stichel et al. 2018), as well as for naturally occurring radionuclides such as ^{210}Pb (Niedermiller & Baskaran 2019, Rigaud et al. 2015), ^{230}Th , and ^{231}Pa (Hayes et al. 2015a, Pavia et al. 2018). The active removal evidenced by these U-series nuclides along the entire 4,000-km length of the plume (**Figure 4a**) to the west of the East Pacific Rise (Niedermiller & Baskaran 2019; Pavia et al. 2018, 2019) suggests that plume-related processes may represent a significant sink for other particle-reactive substances in the deep sea.

The concentration of dFe within the East Pacific Rise plume varied linearly with that of excess ^3He , a conservative tracer of hydrothermal input, from which Resing et al. (2015) and Fitzsimmons et al. (2017) inferred nearly conservative behavior of the dFe as well. If this is true, then the unexpected stability of hydrothermal Fe in the deep sea, whether as colloids or as organic complexes, suggests that this hydrothermal source supplies Fe to the Fe-limited Southern Ocean, where water masses of the density class containing deep-sea hydrothermal plumes outcrop at the surface (Resing et al. 2015, Tagliabue & Resing 2016, Tagliabue et al. 2014a).

Normalizing dFe in the East Pacific Rise plume to ^{228}Ra , rather than excess ^3He , led Kipp et al. (2018) to the very different conclusion that dFe is actively removed from the East Pacific Rise plume with a residence time falling between 9 and 20 years (upper limit 50 years). These apparent inconsistencies can be reconciled by the fact that the linear relationship between dFe and excess ^3He has a large positive excess- ^3He intercept (Fitzsimmons et al. 2017, Resing et al. 2015). An alternative presentation of the same data shows that the ratio of dFe to excess ^3He drops by an order of magnitude over the 4,000-km East Pacific Rise plume (**Figure 6**). For the range of estimated transit times of the plume (25–70 years) (Fitzsimmons et al. 2017), the slope of the relationship in **Figure 6** suggests a half-life of dFe with respect to scavenging and removal of between 7 and 20 years, consistent with the conclusions of Kipp et al. (2018). Although dFe emitted from midocean ridge hydrothermal systems is distributed far more widely than once thought (German et al. 1991, 2016), with a half-life on the order of a decade or two, the hydrothermal dFe is less conservative than initially suggested.

4.1.5. Seafloor processes. Seabed interactions serve as both sources and sinks for TEIs. Sources of dissolved rare earth elements from the seabed have been identified in the Atlantic

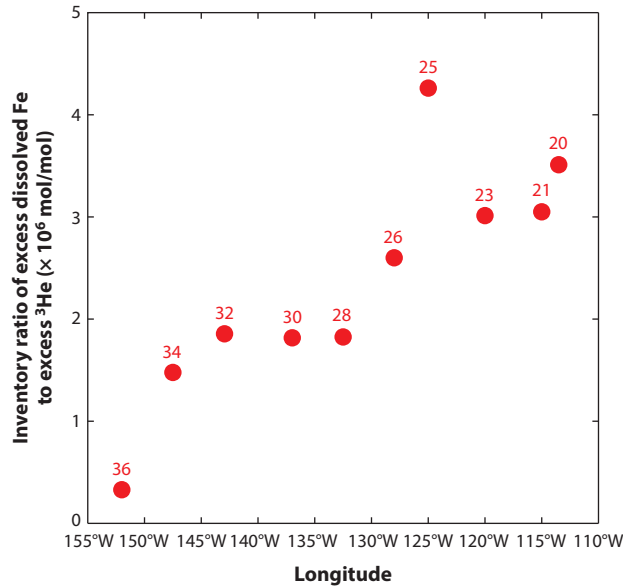


Figure 6

Ratios of the inventory of excess dissolved Fe to the inventory of excess ^3He integrated over the 2,200–2,800-m depth interval, representing the core of the hydrothermal plume, along a zonal section to the west of the East Pacific Rise. The ambient background concentrations subtracted from the measured excess dissolved ^3He and Fe are 0.89 fmol/kg and 0.61 nmol/L, respectively. The numbers above each data point are station numbers, where station 18 was at the crest of the East Pacific Rise and station 36 was at 152°W. Dissolved Fe data are the same as those in **Figure 4** [Conway & John 2014b, Fitzsimmons et al. 2017, Hatta et al. 2015, John et al. 2018, Resing et al. 2015, and unpublished results from K. Bruland, P. Sedwick & J. Wu available in the GEOTRACES Intermediate Data Product 2017 (Schlitzer et al. 2018)]; ^3He data are from Jenkins et al. (2018).

(Stichel et al. 2015, Zheng et al. 2016). Although the majority of the dissolved rare earth elements in deep water of the North Atlantic has been determined to be preformed—i.e., present at the time the water mass entered the basin—a significant fraction (up to tens of percent) has been added from sediments.

Nepheloid layers are persistent features in selected regions of the ocean (Gardner et al. 2018a,b). In some cases, the resuspension of bottom sediments may supply TEIs, as for rare earth elements off the margin of Mauritania (Stichel et al. 2015). The benthic source of dAl seen in **Figure 2e** coincides with a region of strong sediment resuspension (Gardner et al. 2018a,b). Still unresolved is whether the benthic source of Al results from mobilization by sediment resuspension (Measures et al. 2015) or the dissolution of diatom frustules that scavenged dAl from the water column (Middag et al. 2015). These processes are being coded into models and the results compared with observed Al distributions in an effort to resolve their relative contributions (van Hulst et al. 2013, 2014).

In contrast to rare earth elements, and possibly Al, resuspended sediments act as an important sink for particle reactive radionuclides like ^{230}Th and ^{231}Pa (Deng et al. 2014, Hayes et al. 2015a) and ^{210}Pb (Rigaud et al. 2015), as well as for scavenging-prone trace metals like Cu (Jacquot & Moffett 2015). Nepheloid layers can serve as both a source and a sink for Co depending on the characteristics of the resuspended sediments (Noble et al. 2017). Models that include processes associated with nepheloid layers are being tested against distributions of ^{230}Th and ^{231}Pa measured

on GEOTRACES sections (Rempfer et al. 2017, van Hulten et al. 2018) to more generally explore the role of nepheloid layers in the biogeochemical cycles of TEIs.

4.2. Theme 2: Internal Cycling of Trace Elements and Their Isotopes

Internal cycling, broadly defined to encompass all processes that redistribute major ions and TEIs within the ocean, includes biological uptake in surface waters, regeneration from biogenic particles exported to greater depth, abiotic scavenging (both reversible adsorption and irreversible precipitation reactions), and transport by ocean circulation (**Figure 3**). For macronutrients, such as N, Si, and P (**Figure 2a**), and for micronutrients with a long residence times in the ocean, such as Zn (**Figure 2b**) and Cd and Ni (not shown in the figure), circulation plays a dominant role in shaping ocean distributions. Most of the inventory of these species in the deep ocean is preformed, with only minor contributions from local regeneration (Holzer & Brzezinski 2015, Middag et al. 2019, Roshan & Wu 2015c, Sigman & Boyle 2000, Vance et al. 2017, Weber et al. 2018). For TEIs with residence times less than the mixing time of the ocean ($\sim 1,000$ years), local processes of supply and removal dominate their distribution, as seen for Fe (**Figure 2d**) and Co (**Figure 2c**), although internal cycling also influences their distributions, as described below.

4.2.1. Macronutrients. Micronutrient availability limits the biological utilization of macronutrients throughout much of the ocean (Section 1), so the processes controlling macronutrient distributions naturally fall under the purview of GEOTRACES. For example, prominent signals of nitrate utilization ($\delta^{15}\text{N}$ enrichment, primarily in subantarctic waters) and nitrogen fixation ($\delta^{15}\text{N}$ depletion, primarily in subtropical waters) have been traced throughout the upper Atlantic (Marconi et al. 2015, 2019; Tuerena et al. 2015). Marconi et al. (2017) further estimated that 90% of the N fixation in the Atlantic occurs north of 11°S , despite N-fixation-favorable P/N ratios in southern subtropical surface waters, supporting the view that Fe supply by Saharan dust supports N fixation in the Atlantic (Moore et al. 2009).

Nitrate enriched in $\delta^{15}\text{N}$ by denitrification within the southeast Pacific oxygen-deficient zone (ODZ) supplies nitrate to oligotrophic surface waters of the South Pacific subtropical gyre as well as to the upwelling regime off the coast of Peru (Peters et al. 2018). Peters et al. (2018) further used the $\delta^{18}\text{O}$ of nitrate to attribute 50–75% of the heavy $\delta^{15}\text{N}$ signal of nitrate at intermediate depth (500–1,500 m) to regeneration of $\delta^{15}\text{N}$ -enriched organic matter exported from surface waters, and the remainder to mixing of $\delta^{15}\text{N}$ -enriched nitrate directly from areas of denitrification within the ODZ.

Nitrite is an important intermediary in the N cycle within ODZs, where it may represent tens of percent of the bioavailable N. Including nitrite and its isotopes improved the performance of a global ocean N model, as assessed by comparison with GEOTRACES data from the Atlantic and Pacific (Martin et al. 2019).

The Atlantic Meridional Overturning Circulation heavily influences both the distribution and isotopic composition of dSi in the Atlantic, reflecting the distinct isotopic signature of Si derived from Arctic (heavy) and Antarctic (light) regions (Brzezinski & Jones 2015). Modeling these distributions has enabled discrimination between preformed and regenerated pools on a global scale and identified most of the dSi in the deep ocean as preformed and with a Southern Ocean origin (Holzer & Brzezinski 2015).

4.2.2. Biological uptake and regeneration. Micronutrient uptake by organisms can be estimated by combining their cell quotas, expressed as ratios of metal to either C or P (Twining & Baines 2013), with their growth rates (Lis et al. 2015). A comparison of cell quotas with the

metal-to-P ratios of labile phases leached from bulk particulate material indicated that particulate Zn (pZn), pCu, pNi, and pCo are associated mainly with cellular material in surface waters of the North Atlantic (Twining et al. 2015). Export of these biogenic particles causes the observed surface depletion of micronutrient concentrations.

Evaluation of biological uptake and retention of Fe in regimes with contrasting persistently low versus seasonally high inventories of dFe led to the surprising discovery that the biotic Fe inventories were similar in the two systems near New Zealand (Boyd et al. 2015). Furthermore, Fe recycling efficiency quadrupled as dFe inventories were depleted over time, indicating that Fe recycling was adjusted by the ecosystem to maintain the biotic Fe pool. A possible strategy to control Fe retention was identified in the GEOTRACES study off Peru, where the concentrations of certain Fe-binding ligands were five times higher in high-nitrate, low-Fe waters offshore than in recently upwelled high-nitrate, high-Fe waters nearshore, or in low-nitrate waters of the South Pacific subtropical gyre (Boiteau et al. 2016a), suggesting a biological response to retain growth-limiting Fe.

Export of particulate material from surface waters integrates the combined effects of biological uptake and regeneration. Export fluxes evaluated during many GEOTRACES cruises using the ^{234}Th – ^{238}U radioactive disequilibrium approach (Anand et al. 2018, Black et al. 2018, Lemaitre et al. 2018, Owens et al. 2015, Planchon et al. 2015, Puigcorb  et al. 2017) span a range of micronutrient conditions. For example, Planchon et al. (2015) reported that export fluxes of particulate organic carbon (POC) from naturally Fe-fertilized waters downstream of the Kerguelen Archipelago (Bowie et al. 2015) were two to five times the export flux from the unfertilized upstream region, demonstrating the potential for Fe fertilization to enhance the efficiency of the biological pump in high-nutrient, low-chlorophyll waters of the Southern Ocean.

Fluxes of pCd, pMn, and pCo from surface waters were estimated using the ^{234}Th method along the GEOTRACES transect between Peru and Tahiti (Black et al. 2019). Loss of these metals from surface waters by export was balanced by mixing from sources at the coast, as inferred from their measured concentrations in surface waters and lateral mixing rates derived from the distribution of ^{228}Ra (Sanial et al. 2018). Aerosol deposition represented an insignificant source of these metals in this region.

Exported Fe is subject to both regeneration and further scavenging in the thermocline. In some areas well away from margin sediments, where reductive mobilization introduces isotopically light dFe (Section 4.1.3), regeneration of biogenic Fe is evident in the light isotopic composition of dFe in intermediate waters (Abadie et al. 2017), reflecting the preferential uptake of light dFe by phytoplankton (Ellwood et al. 2015). Regeneration is also evident from the linear relationship between dFe and apparent oxygen utilization that has been observed in many regions (Sunda 1997). Regenerated Fe/C ratios estimated from GEOTRACES studies in the Atlantic range from approximately 3 $\mu\text{mol/mol}$ in the tropical South Atlantic (Rijkenberg et al. 2014) to approximately 7 $\mu\text{mol/mol}$ in the subtropical North Atlantic (Fitzsimmons et al. 2015b, Hatta et al. 2015), although the differences among these studies result more from the coefficients used to convert apparent oxygen utilization to C respired than from the measured relationships between dFe and apparent oxygen utilization. In either case, these Fe/C regeneration ratios fall well below the cell quotas reported for the subtropical North Atlantic (30–60 $\mu\text{mol/mol}$, varying among taxa) (Twining et al. 2015), suggesting that 60–90% of the biogenic Fe exported from surface waters either is not regenerated or is removed by scavenging soon after being regenerated (Hatta et al. 2015).

A strong correlation between dCd and phosphate was evident in the earliest data (Boyle et al. 1976, Bruland et al. 1978a), suggesting nutrient-like behavior even though Cd had no known biological function in marine plankton at the time. GEOTRACES studies have now shown that the uptake, export, and regeneration of Cd are tightly coupled with those of P (Black et al. 2019).

Within nutrient-rich waters at high latitudes, Cd/P uptake ratios are much greater than they are in oligotrophic low-latitude waters (Baars et al. 2014, Middag et al. 2018, Quay & Wu 2015, Quay et al. 2015). Ratios of pCd to pP exported at high latitudes are on average more than double the ratios at low latitudes (Quay et al. 2015), and in some cases differences as great as an order of magnitude have been reported (Bourne et al. 2018). Preferential uptake of Cd at high latitudes, especially in the Southern Ocean, is thought to reflect a combination of greater concentration of bioavailable Cd there (resulting from higher dCd concentrations together with reduced complexation by organic ligands) and the enhanced uptake of Cd under conditions of growth limitation by Fe and/or other micronutrients (Baars et al. 2014).

Throughout the deep ocean, dCd occurs predominantly as a preformed constituent (Baars et al. 2014, Middag et al. 2018, Quay & Wu 2015, Roshan & Wu 2015b, Roshan et al. 2017). Regenerated Cd contributes more to total dCd at shallower depths, approaching 50% above 1,000 m in the North Atlantic and generally dominating the dCd above approximately 300 m (Quay & Wu 2015, Roshan et al. 2017). The kink in the dCd/dP relationship that has been evident since the earliest high-quality data were gathered (Boyle et al. 1976) is now understood to be caused by the mixing of deep water masses that contain differing preformed Cd/P ratios (Baars et al. 2014, Middag et al. 2018, Quay & Wu 2015, Quay et al. 2015, Xie et al. 2015) enhanced by an overprint at shallower depths by the addition of regenerated Cd and P at a lower Cd/P ratio in low latitudes (Quay & Wu 2015, Roshan et al. 2017).

One exception to the biological control of the internal cycling of Cd is the enhanced uptake of Cd by particles in low-oxygen environments, where sulfide generation within anoxic interstitial pore fluids of aggregates can lead to CdS precipitation (Conway & John 2015, Janssen et al. 2014). However, Ohnemus et al. (2017) reported that sulfide phases seem to be unimportant as a carrier for pCd in the ODZ off Peru. Future studies will need to resolve the contribution of sulfide precipitation in particulate microenvironments to the marine biogeochemical cycle of Cd.

The distribution of Co, like that of Fe, is influenced both by biological uptake and regeneration and by abiotic scavenging. In subtropical North Atlantic surface waters, pCo is associated mainly with cell material, indicating the importance of biological uptake (Twining et al. 2015). Mass balance calculations find that Co is recycled multiple times within the euphotic zone before being exported, much as is the case for macronutrients (Dulaquais et al. 2014a). Vertical profiles of dCo and their positive correlation with dP in the upper water column are further indications of biological uptake in the euphotic zone, export, and regeneration in subsurface waters (Dulaquais et al. 2014a; Hawco et al. 2016; Noble et al. 2012, 2017; Saito et al. 2017). pCo is correlated with pP, and both, in turn, are correlated with chlorophyll in the upper water column along a transect between Peru and Tahiti (Hawco et al. 2016). Stoichiometric relationships between dCo and dP evolve with depth in the North Atlantic, a feature that is attributed to the interleaving of water masses bearing different preformed dCo/dP ratios upon which is superimposed the transition from a regeneration-dominated supply of dCo in the upper thermocline to scavenging-dominated removal of dCo at greater depths (Saito et al. 2017).

The affinity of Co for scavenging onto Mn oxides is evident within the oxic thermocline west of 100°W along the Peru–Tahiti transect, where a secondary pCo maximum occurred between depths of 300 and 500 m, well below the primary pCo maximum in the euphotic zone, and coinciding with a pMn maximum (Hawco et al. 2016). Photoreduction of Mn(IV) inhibits scavenging of Co by Mn oxides within the euphotic zone, while slow kinetics of Mn oxidation within low-oxygen waters of the thermocline off Peru inhibited scavenging of Co by Mn oxides there as well (Hawco et al. 2016). Stronger scavenging of dCo is evident in the oxic thermocline west of 100°W, where ²³⁴Th-derived fluxes of pCo and pP are consistent with the interpretation of dCo/dP ratios in identifying a transition from control of Co distributions by biological uptake and regeneration

in the upper ~200 m to control by scavenging, predominantly involving Mn oxides, at greater depths (Black et al. 2019, Hawco et al. 2016).

Scavenging and removal of Co are responsible for the general pattern of decreasing dCo concentrations with depth in the deep ocean (**Figures 2c** and **5**). Scavenging is also responsible for the general trend of decreasing dCo concentration with distance (water mass age) along the deep ocean conveyor flow path from the Atlantic to the Pacific, which Hawco et al. (2018) interpreted to estimate a residence time of dCo in the deep sea of approximately 1,000 years. Although dCo concentrations are lower in the deep ocean than they are at intermediate depths (**Figures 2c** and **5**), removal of dCo is also much slower in the deep ocean. Hawco et al. (2018) estimated that more than 50% of the Co buried in deep-sea sediments is scavenged from depths above 500 m, where the residence time of dCo is on the order of decades. Greater dCo concentrations at intermediate depths (**Figures 2c** and **5**), despite much greater rates of removal there, reflect the importance of Co mobilization from shelf and upper-slope sediments in shaping the distribution of dCo in the ocean. Model results are generally consistent with this empirical approach, indicating that most of the supply of dCo to the ocean derives from mobilization out of shelf and upper-slope sediments, with a residence time of approximately 250 years for the global ocean and only 7 years for the upper 250 m (Tagliabue et al. 2018).

The tight coupling between the distributions of dZn and dSi in the ocean has puzzled oceanographers since it was first discovered (Bruland et al. 1978b). Zn is associated primarily with the organic components of cells (Twining & Baines 2013, Twining et al. 2014) rather than with diatom frustules (Ellwood & Hunter 2000). A positive linear correlation between dZn and dSi is generally observed worldwide (Roshan et al. 2018, Weber et al. 2018), although departures from the global trend have been observed in hydrothermal plumes (Roshan et al. 2016), within the Mediterranean outflow into the North Atlantic (Roshan & Wu 2015a), and in North Pacific waters, where regeneration of Zn-rich particles has been inferred (Kim et al. 2017).

As in the case of Cd, Zn/P uptake ratios at high latitudes are much greater than those at low latitudes (Middag et al. 2018, Wyatt et al. 2014), possibly by as much as an order of magnitude (Roshan et al. 2018). Consequently, Zn is efficiently stripped from surface waters in the Southern Ocean, leaving low Zn/P ratios in the mode and intermediate waters that ventilate the thermocline (Wyatt et al. 2014), similar to the conditions that impart a low Si/P ratio to these waters (Sarmiento et al. 2004). Noting that surface waters depleted in both Zn and Si ventilate the thermocline, while mixing of regenerated Zn and Si at depth around Antarctica imprints deep waters with elevated concentrations of both before spreading northward into the other ocean basins, Vance et al. (2017) hypothesized that the global relationship between Zn and Si can be explained largely by mixing of these water mass end members.

A competing hypothesis invokes reversible scavenging of dZn to account for the observed Zn–Si correlation together with the regeneration of Zn at greater depth than for P (John & Conway 2014). Although biological uptake preferentially consumes the light isotopes of Zn (Conway & John 2014a, Samanta et al. 2017), the observed surface enrichment of dZn in light isotopes indicates that processes other than biological uptake must contribute to Zn removal (John & Conway 2014). Laboratory studies had shown that abiotic adsorption to biogenic particles preferentially scavenges heavy isotopes, which served as the basis for the hypothesis invoking scavenging as an important process removing Zn from surface waters and desorption of scavenged Zn to account for its overall greater depth of regeneration (John & Conway 2014).

GEOTRACES data provide evidence in support of both hypotheses. Using optimum multi-parameter approaches, Roshan & Wu (2015c) and Middag et al. (2019) estimated that virtually all of the dZn in the deep Atlantic is preformed, consistent with the hypothesis of Vance et al. (2017). Roshan et al. (2018) reached somewhat different conclusions; their model required downward

transfer of regenerated Zn via reversible scavenging to match the observed enrichment of dZn at depth in addition to comparable regeneration in the upper thermocline, as for P at low latitudes.

Weber et al. (2018) reached conclusions generally similar to those of Roshan et al. (2018) using a diagnostic model of Zn biogeochemistry. Observed dZn distributions could be reproduced better with a model-optimized scavenging parameter than when simulating the mixing hypothesis of Vance et al. (2017). Their optimized model results indicated that 65–70% of the dZn in the deep North Pacific is preformed, while 15–20% each is delivered by desorption of scavenged Zn and by regeneration of biogenic Zn, the latter being greater at shallow depths and the former being greater in bottom waters. Their model also successfully reproduced the observed profiles of $\delta^{66}\text{Zn}$ of dZn in both the Atlantic and the Pacific.

Although substantial progress has been made in our knowledge of the biogeochemical cycle of Zn in the ocean, disagreements among the studies cited above identify needs for further investigation. As for Cd (Roshan et al. 2017), additional constraints on the preformed Zn concentrations and Zn/P ratios at high latitudes will improve the ability to discriminate between preformed and regenerated Zn in deep waters and, by difference, thus evaluate the contributions by regeneration and/or desorption of metals transported downward from shallower depths.

4.2.3. Chemical speciation and physical form. The bioavailability of micronutrients and their tendency to be removed by abiotic scavenging processes are influenced strongly by the chemical speciation and physical form of the element (Boyd & Tagliabue 2015, Boyd et al. 2017, Hutchins & Boyd 2016, Lis et al. 2015, Tagliabue et al. 2017). Micronutrient elements occur in the ocean primarily in the form of strong organic complexes, which have very different biogeochemical properties from those of free inorganic species (Bruland et al. 2014). Modeling studies have found that the distributions of micronutrients cannot be reproduced without incorporating ligands and their impact on an element's properties. These models are most advanced for Fe, and clearly demonstrate the importance of ligands in shaping the distribution of Fe in the ocean (Frants et al. 2016, Pham & Ito 2018, Tagliabue & Resing 2016, Tagliabue et al. 2014b, Völker & Tagliabue 2015) and the role of Fe in the ocean carbon cycle (Tagliabue et al. 2014a). Although they are at an earlier stage of development, models also indicate the importance of ligands in shaping the distributions of Co (Tagliabue et al. 2018) and Zn (Weber et al. 2018).

4.2.3.1. Ligands. Despite the recognized importance of ligands, their sources, sinks, and structures remain largely unknown (Bundy et al. 2016, Gledhill & Buck 2012). With a few exceptions where the structural identity of ligands has been determined (Boiteau et al. 2016a,b, 2019; Mawji et al. 2008), the concentrations and binding constants of ligands are determined by electrochemical methods that provide no further information about ligand composition. Furthermore, different electrochemical technologies have been employed to determine ligand concentration and binding constants (Bruland et al. 2014), leaving open questions about the comparability of the methods.

Recognizing the importance of ligands for TEI biogeochemistry and the implications for understanding the role of micronutrients in regulating the ocean C cycle, GEOTRACES investigators helped form a SCOR-sponsored working group (working group 139) to examine the methods used in ligand research. Findings to date have been published in two special volumes (for overviews, see Buck et al. 2017, Lohan et al. 2015). In addition, to ensure the consistency of results obtained by various methods, GEOTRACES has ongoing efforts at intercalibration, just as for TEIs, including the analysis of replicate samples by different laboratories (Buck et al. 2012) and the comparison of data from crossover stations that are sampled on more than one expedition (Buck et al. 2016).

Distributions of Fe-binding ligands reveal qualitative information about their sources and sinks in the ocean. Fe-binding ligands are ubiquitous in the ocean and, with a few exceptions (e.g., hydrothermal plumes; Buck et al. 2015), their concentrations exceed those of dFe (Buck et al. 2015, 2018; Gerringa et al. 2015). As reported in previous studies (Boyd & Tagliabue 2015, Gledhill & Buck 2012), concentrations of Fe-binding ligands were greatest in surface waters along GEOTRACES sections, often corresponding to the depth of maximum chlorophyll abundance, indicating production by phytoplankton (Buck et al. 2015, Gerringa et al. 2015). An additional source is suggested by increased ligand concentrations in upper-thermocline regions of intense POC regeneration (Buck et al. 2018), consistent with the results of incubation experiments showing siderophore production from decomposing particles (Boyd & Tagliabue 2015, Boyd et al. 2010, Velasquez et al. 2016). Binding constants of ligands produced during POC regeneration tend to be lower than those produced by phytoplankton in surface water (Boyd & Tagliabue 2015). Benthic sources of Fe-binding ligands have been inferred from near-bottom increases in ligand concentrations in the Atlantic (Buck et al. 2015) and Pacific (Buck et al. 2018), in the California Current (Boiteau et al. 2019), and in the Mediterranean Sea (Gerringa et al. 2017).

There is limited evidence to constrain the residence time of ligands in the ocean, but a few clues suggest a relatively long lifetime for Fe-binding ligands in the deep sea and a much more dynamic cycle in surface water. Gerringa et al. (2015) interpreted a southward decrease in ligand concentrations within North Atlantic Deep Water as reflecting a turnover time of approximately 1,000 years. By contrast, daily sampling at the Hawaii Ocean Time-Series station revealed a one- to two-day lag in ligand concentration following variability in dFe, suggesting rapid production of ligands in response to Fe supply and similarly rapid destruction by photodecomposition (Fitzsimmons et al. 2015c).

To further characterize the form of ligands in surface waters, Fitzsimmons et al. (2015a) reported that approximately 80% of the operationally defined dFe in surface waters of the subtropical North Atlantic occurs as colloids, consistent with previous studies, whereas approximately 75% of the Fe-binding ligands were recovered in the soluble (<10 kDa) fraction. This difference was unexpected, given that dFe is thought to occur as organic complexes. The authors offered two hypotheses to reconcile the observations: either (a) their method failed to detect colloidal ligands, or (b) a large fraction of the colloidal Fe (cFe) occurs in inorganic phases. These hypotheses remain to be tested.

Boyd & Tagliabue (2015) interpreted the spatial distribution and binding characteristics of Fe-binding ligands to indicate that the strongest ligands are produced opportunistically in surface waters, perhaps by bacteria, in response to a transient Fe supply or other need. Results from the GEOTRACES Peru–Tahiti section support this view (Boiteau et al. 2016a). Hydrophilic ferrioxamine siderophores were most abundant in waters with low Fe stress, whereas in waters with greater Fe stress (low Fe/N ratios), amphiphilic siderophores (amphibactins) were more abundant, possibly produced as a strategy to retain Fe while exploiting available macronutrients. Boiteau et al. (2019) reported results from a study of the California Current consistent with the observations from waters off Peru. Ferrioxamines were more abundant in recently upwelled Fe-rich water, whereas amphibactins were more abundant in waters with low Fe/N ratios. The authors suggested that the abundances and ratios of siderophore compounds may be used in future studies as a probe of Fe limitation and to provide insight into ecological strategies for managing Fe under diverse environmental conditions.

Large stability constants for Co–ligand complexes ($\log K > 16.8$; Saito et al. 2005) complicate both observations and modeling of Co (Noble et al. 2012, 2017; Tagliabue et al. 2018). Co in surface waters occurred entirely in the form of strong organic complexes (Hawco et al. 2016, Noble et al. 2017), consistent with prior studies, which have also reported the production of these strong

ligands by cyanobacteria (Saito et al. 2005). Deeper in the water column, a substantial fraction of dCo occurs in a labile form, indicating the presence of either free inorganic species or Co-binding ligands with much smaller stability constants (Hawco et al. 2016; Noble et al. 2012, 2017).

Cu is also bound by strong organic complexes (Coale & Bruland 1990). Stability constants tend to be smaller for Cu than for Co but greater than those for Cd and Zn (Jacquot & Moffett 2015). Stability constants of Cu ligands determined in GEOTRACES studies tend to decrease from north to south. Cu-binding ligands have log K values between 15 and 16.5 in the northeast Pacific (Whitby et al. 2018) and approximately 13 in the subtropical North Atlantic (Jacquot & Moffett 2015), the eastern tropical South Pacific (Boiteau et al. 2016b), and the Tasman Sea (Thompson et al. 2014), while the lowest values (~ 11.8) are in the Southern Ocean (Heller & Croot 2015). An intriguing feature that is yet to be explained is that the stability constants for Cu-binding ligands are approximately an order of magnitude larger in upwelling waters off eastern boundary current regions of Mauritania (Jacquot & Moffett 2015) and Peru (Boiteau et al. 2016b) than offshore at similar latitudes.

Speciation has been studied less within GEOTRACES for Zn than for other micronutrients discussed above. Within the Tasman Sea, concentrations of Zn-binding ligands fall in the range 0.2–4 nmol/kg, generally in excess of the dZn concentrations (Sinoir et al. 2016), and Zn ligands have stability constants with log K values between 9.3 and 11.4. The maximum concentrations of Zn-binding ligands coincide with a maximum in $\delta^{66}\text{Zn}$ of dZn (Samanta et al. 2017, Sinoir et al. 2016), leading to the suggestion that the Zn-binding ligands are produced by eukaryotic phytoplankton.

At high latitudes, both in the North Pacific (Kim et al. 2015) and in the Southern Ocean (Baars & Croot 2011), concentrations of dZn often exceed concentrations of Zn-binding ligands due to high concentrations of dZn in recently upwelled water. Baars & Croot (2011) suggested that high concentrations of free Zn in the Southern Ocean account for the very large Zn/P uptake ratios there.

Information about ligand distributions and their metal-binding characteristics generated during GEOTRACES is helping to constrain their sources (phytoplankton, continental runoff, and sediments) and sinks (microbial degradation and photodecomposition). This information can inform the design of future studies to more completely characterize the processes that regulate the production and loss of ligands in the ocean, as well as the rates of those processes.

4.2.3.2. Colloids. A large fraction of the operationally defined dFe in the ocean occurs as colloids (von der Heyden & Roychoudhury 2015). Therefore, characterizing the marine biogeochemistry of Fe requires examining the properties of colloids (Tagliabue et al. 2017).

Most of the dust-derived dFe in the ocean seems to be introduced in cFe. This is evident in aerosol leaching studies (Aguilar-Islas et al. 2010, Fishwick et al. 2014) and in the global pattern of observations that indicate that cFe constitutes a much larger fraction of dFe in surface waters that receive large supplies of dust than in low-dust regions. For example, in North Atlantic waters underlying the Saharan dust plume, approximately 80% of the surface dFe occurs as cFe (Fitzsimmons & Boyle 2014, Fitzsimmons et al. 2015b). By contrast, in low-dust regions of the Southern Ocean, cFe has been reported to contribute $23\% \pm 11\%$ (Chever et al. 2010) to $37\% \pm 8\%$ (Boye et al. 2010) of the dFe (for additional examples, see Boye et al. 2010, Fitzsimmons et al. 2015b).

Aerosol-derived cFe may be solubilized by strong Fe-binding ligands (Fishwick et al. 2014). However, despite the presence of strong Fe-binding ligands in the surface ocean, stable isotope measurements indicate that cFe in the subtropical North Atlantic is not sufficiently solubilized by ligands to achieve exchange equilibrium with soluble Fe (sFe). Fitzsimmons et al. (2015b) reported

much larger $\delta^{56}\text{Fe}$ values for sFe (+1.5‰) than for cFe (+0.5‰). Both forms of Fe are heavier than bulk pFe from the same location ($\sim 0.08\text{‰}$) (Revels et al. 2015). These results are consistent with preferential biological removal of light sFe (Ellwood et al. 2015), enriching sFe in heavy isotopes, together with partial exchange between sFe and cFe (Fitzsimmons et al. 2015b). Whether a portion of the cFe occurs in nonexchangeable form or the timescale for isotope equilibrium exceeds the residence time of Fe in the surface ocean has yet to be investigated.

Despite the abundance of cFe in surface waters, very little exists within the deep chlorophyll maximum either in the North Atlantic (Fitzsimmons & Boyle 2014, Fitzsimmons et al. 2015b) or in the subtropical North Pacific (Fitzsimmons et al. 2015c). Either cFe is consumed by the organisms in the deep chlorophyll maximum, possibly as a strategy to deal with Fe stress, or cFe is aggregated into filterable particles.

At greater depths, dFe often partitions in approximately 50:50 proportions between cFe and sFe (Boye et al. 2010, Fitzsimmons et al. 2015b). Similar $\delta^{56}\text{Fe}$ values in cFe and sFe samples recovered from depth are consistent with an exchange equilibrium between the two phases (Fitzsimmons et al. 2015b). An exception to this 50:50 partitioning in deep water was observed in the western North Atlantic, especially in Labrador Sea Water, where elevated dFe concentrations were enriched in cFe (Fitzsimmons et al. 2015b). dFe along the western margin has an isotopic composition indicative of nonreductive mobilization from sediments (Conway & John 2014b), and elevated ^{228}Ra concentrations indicate recent contact with sediments (Charette et al. 2015), suggesting a source of cFe from the seabed.

4.2.3.3. Particles. The composition of particulate material informs us about the processes that generate or introduce the particles as well as about their role in the biogeochemistry of TEIs. For example, the association of Fe(II) with organic matter in surface waters of the Weddell Sea (von der Heyden et al. 2012) and off Peru (Heller et al. 2017) may reflect a predominantly biogenic source for this pFe. In contrast to these surface waters, within the ODZ off Peru most of the pFe occurs as Fe(III). Detection of lepidocrocite in these samples was interpreted to indicate that the Fe(III) had been formed via oxidation of dissolved Fe(II) using nitrite as the electron acceptor (Heller et al. 2017).

The elemental stoichiometry of particles also provides valuable clues to their origin. For example, by comparing cell quotas (metal/P ratios) of various taxa recovered from surface waters of the subtropical North Atlantic with element ratios in the leachable phases of bulk particulate material, Twining et al. (2015) demonstrated that the pZn, pCu, pNi, and pCo are associated mainly with cellular material, whereas 70% of the pFe and pMn are associated with other authigenic phases, presumably oxyhydroxides. Within a depth interval of elevated bacterial abundance coinciding with the upper ODZ off Peru, metal/P ratios (for Cd, Co, Cu, Ni, V, and Zn) were several times greater than those in the phytoplankton-dominated surface waters above, suggesting that bacteria may play an important role in the cycling of these elements, at least within ODZ regimes (Ohnemus et al. 2017). Statistical relationships among particulate element concentrations along the entire section from Peru to Tahiti (Lee et al. 2018) revealed regular associations between trace elements and major phases: lithogenic (Al, Ti, and Fe), biogenic (P, Cd, Co, Cu, Ni, and V), Mn oxide (Mn and Co), and mixed oxyhydroxide (Fe, V, P, Ni, Cu, and, in low-oxygen waters, Cd and Co).

A substantial portion of the pFe collected on GEOTRACES cruises occurred in a labile, or leachable, form, ranging from 25% to 30% in the subtropical North Atlantic (Milne et al. 2017, Revels et al. 2015) to more than 50% along most of the section between Peru and Tahiti (Marsay et al. 2018). The $\delta^{56}\text{Fe}$ of the leachable pFe tends to be less than that of either the bulk pFe or dFe, which has been interpreted to indicate a contribution to the leachable Fe from dFe(II) reductively mobilized from sediments (Marsay et al. 2018, Revels et al. 2015). Concentrations of leachable pFe

are correlated with concentrations of dFe in the eastern Atlantic, leading Milne et al. (2017) to conclude that the leachable pFe remains in a labile form that can serve to buffer the concentration of dFe against other processes of supply or removal.

4.2.4. Scavenging, particle dynamics, and residence times. For the study of scavenging and particle dynamics, Th has an advantage over other particle-reactive radionuclides (e.g., ^{210}Pb and ^{231}Pa) because it has multiple radiogenic isotopes with half-lives ranging from 24 days (^{234}Th) to 75,000 years (^{230}Th). Simultaneous equations containing rate constants for the various components of scavenging, including adsorption, desorption, particle decomposition, and settling, can be written for each Th isotope (Bacon & Anderson 1982). Using data for three Th isotopes (^{228}Th , ^{230}Th , and ^{234}Th) from the subtropical North Atlantic, Lerner et al. (2017) first demonstrated that a one-dimensional mass balance for ^{230}Th holds (i.e., that net lateral transport is negligible), a necessary condition when using Th isotopes to constrain particle dynamics. They were then able to constrain each of the rate constants identified above.

In a follow-up study of the same region, Lerner et al. (2018) tested the sensitivity of the adsorption rate constant to the major phase composition of particles, including biogenic ($\text{CaCO}_3 + \text{opal} + \text{POC}$), lithogenic, Mn oxyhydroxide, and Fe oxyhydroxide phases as the master variables. They reported that the adsorption rate constant varied most closely with the abundance of biogenic particles within the productive upwelling system off northwest Africa, whereas the covariance with Mn oxyhydroxides was greater at stations farther to the west. These insights concerning scavenging processes and particle dynamics derived from GEOTRACES studies are being incorporated into ocean models of ^{231}Pa and ^{230}Th (Dutay et al. 2015, Rempfer et al. 2017, van Hulst et al. 2018), with the eventual goal of incorporating these parameters into models for a broader suite of TEIs.

One metric of our overall understanding of the processes that regulate the biogeochemical cycle of an element is the ability to code that information into a model and predict the element's residence time. Tagliabue et al. (2016) examined this metric during the first Fe model intercomparison project, which compared the products of 13 global ocean models. Because each of the models was tuned to give an inventory of dFe in the ocean similar to that constrained by GEOTRACES data, the total supply of Fe to the ocean scales linearly with its residence time. Consequently, the two-orders-of-magnitude range of residence times among models provides a measure of the uncertainty in the rate of supply of dFe to the ocean (**Figure 7**).

New information generated by GEOTRACES studies is improving our knowledge of the processes that regulate TEI distributions and the rates of those processes. For example, ^7Be has been used to estimate the fluxes of aerosol-associated TEIs to the ocean (Kadko et al. 2019). Ra isotopes are being used increasingly to evaluate sources of TEIs at ocean margins (Black et al. 2019, Charette et al. 2016, Sanial et al. 2018).

Long-lived Th isotopes are also employed to quantify the supply of dissolved TEIs from aerosols. The residence time of dFe in the surface ocean estimated following this approach was 6–12 months at the Hawaii Ocean Time-Series station (Hayes et al. 2015b) and 1–2 months at the Bermuda Atlantic Time-Series Study station (Hayes et al. 2018a). The difference in residence times was attributed to the greater flux of dust to the North Atlantic, as well as to greater retention of Fe by the more Fe-stressed ecosystem in the Pacific. Hayes et al. (2018a) used this approach to estimate the dust supply of other TEIs.

Fluxes and residence times can be also be quantified by pairing concentrations of particulate TEIs with concentrations of particulate ^{230}Th . First applied to estimate dust fluxes in the eastern North Atlantic (Anderson et al. 2016), this approach was subsequently used to calculate fluxes of POC, P, and several trace elements. These ^{230}Th -normalized fluxes agree particularly well with

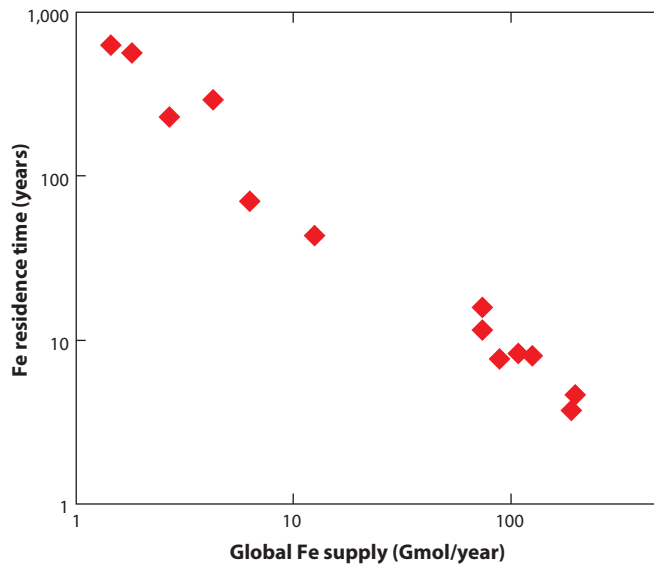


Figure 7

Results from 13 ocean models containing the biogeochemical cycle of Fe, illustrating the relationship between the residence time of dissolved Fe in the ocean and its global average rate of supply (Tagliabue et al. 2016). The range of values shown here illustrates the uncertainty in the rate of supply of Fe to the ocean.

average annual fluxes collected by sediment traps of the Ocean Flux Program, deployed near Bermuda, for POC, P, Cd, and Cu (Hayes et al. 2018b). Building on these early successes, the ^{230}Th approach is now being developed to evaluate fluxes and regeneration length scales of POC on GEOTRACES sections (Pavia et al. 2019).

4.3. Theme 3: The Development of Proxies for Past Change

Geochemical proxies used in paleoceanography represent one of the major themes of GEOTRACES because many of the TEIs employed in the study of modern ocean processes also serve as indicators of ocean conditions in the past. The proxies studied most widely in GEOTRACES include N isotopes, ^{230}Th , ^{231}Pa , and Nd isotopes. Information gained about the biogeochemical cycles of these tracers in the modern ocean will lead to more reliable interpretation of their paleoceanographic records. Other TEIs studied in the investigation of modern ocean processes may also find future applications in paleoceanography as the processes and environmental conditions that shape the tracer in the modern ocean become better established.

Studies of N isotopes ($\delta^{15}\text{N}$ of nitrate) measured along GEOTRACES sections in the Atlantic (Marconi et al. 2015, 2017, 2019; Tuerena et al. 2015) agree that individual water masses have distinctive isotopic signatures that reflect the sum of their preformed properties together with the signals imparted by nitrate utilization (most significantly in subantarctic waters) and N fixation (primarily north of 11°S). Synthesis of these results to identify implications for paleoceanographic studies has yet to be completed.

Distributions of dissolved ^{230}Th and ^{231}Pa measured along GEOTRACES sections throughout the Atlantic (Deng et al. 2014, 2018; Hayes et al. 2015a) fail to show the foundational principle of a simple relationship with water mass age to enable sedimentary $^{231}\text{Pa}/^{230}\text{Th}$ ratios to be used as a proxy for the strength of Atlantic Meridional Overturning Circulation (Henderson & Anderson 2003). Although mass balance calculations confirm a net southward export of dissolved ^{231}Pa from

the Atlantic (Deng et al. 2018), other factors, such as regional variability of scavenging intensity, have a greater effect on the dissolved $^{231}\text{Pa}/^{230}\text{Th}$ ratio. Ongoing synthesis of these findings is directed toward better definition of conditions under which sediment $^{231}\text{Pa}/^{230}\text{Th}$ ratios can be used to assess past changes in the strength of the Atlantic Meridional Overturning Circulation.

The use of ^{230}Th as a constant-flux proxy to evaluate preserved fluxes of sedimentary constituents relies on the assumption of a closed one-dimensional mass balance where the flux of ^{230}Th to the seabed at any location is equal to its rate of production by ^{234}U decay in the overlying water column. Detailed analysis of ^{230}Th scavenging dynamics in the Atlantic confirms that the required mass balance generally holds (Lerner et al. 2017), with a maximum departure from a closed one-dimensional mass balance occurring in productive waters off the coast of northwest Africa, where boundary scavenging leads to a net lateral supply of dissolved ^{230}Th from the oligotrophic gyre (Hayes et al. 2015a).

A fundamental issue underlying the use of Nd isotope (ϵ_{Nd}) signals archived in sediments to constrain past changes in the end-member provenance of deep waters is the degree to which the isotopic composition of dNd behaves conservatively as dNd is mixed throughout the ocean. A synthesis that compared ϵ_{Nd} against conservative circulation tracers obtained promising results, concluding that the distribution of ϵ_{Nd} in the modern ocean is influenced mainly by water mass mixing in the deep sea when at distances more than 1,000 km from ocean margins (Tachikawa et al. 2017). Other studies reported consistent results for the Atlantic (Garcia-Solsona et al. 2014) and Pacific (Basak et al. 2015) sectors of the Southern Ocean.

The long-term stability of the ϵ_{Nd} composition of water mass end members is also implicit in the use of ϵ_{Nd} to reconstruct the provenance of water masses in the past. Lambelet et al. (2016) defined the ϵ_{Nd} of the main components of North Atlantic Deep Water, where Labrador Sea Water has much lower ϵ_{Nd} than the other contributing sources (Iceland–Scotland Overflow Water and Denmark Strait Overflow Water). Different bottom water masses formed around Antarctica (Adélie Land, the Weddell Sea, and the Ross Sea) also have distinct ϵ_{Nd} signatures, but the differences among these sources is less than the differences among the components of North Atlantic Deep Water (Lambelet et al. 2018).

Studies along GEOTRACES sections in the North Atlantic (Stichel et al. 2015) and South Atlantic (Zheng et al. 2016) reported evidence for sedimentary sources of dNd. Although the initial assessment suggests that these sources may have a minor impact on the use of ϵ_{Nd} as a water mass provenance proxy, a more complete assessment awaits a synthesis of the growing database from GEOTRACES expeditions.

Novel isotope systems with potential applications in paleoceanography are also being investigated in GEOTRACES. For example, Ba isotopes may find application in studies of the strength and/or efficiency of the biological pump (Horner et al. 2015, Hsieh & Henderson 2017). Cd isotopes are being assessed as a metric for nutrient utilization, with possible application to studies of past changes in the efficiency of the ocean's biological pump (Abouchami et al. 2011, Janssen et al. 2019, Xie et al. 2015). Developmental work on Cr isotopes, potentially a tracer for past ocean redox conditions, is also underway (Moos & Boyle 2019, Scheiderich et al. 2015).

5. FUTURE TRAJECTORIES OF RESEARCH ON TRACE ELEMENTS AND THEIR ISOTOPES

5.1 . Process Studies

A philosophical principle embedded in the design of GEOTRACES was that results from a global survey would reveal unexpected features in TEI distributions, indicating an influence by one or more processes that were not understood. These features would then logically serve as targets for

future studies that would more thoroughly characterize the processes involved. Several examples can be identified from the results described in this review, the goals of which include the following:

1. Quantify preformed concentrations of TEIs in water mass source regions and the processes regulating these concentrations to permit more precise calculation of their regenerated components throughout the ocean.
2. Identify the conditions that cause certain micronutrients to be consumed preferentially relative to P within nutrient-rich surface waters.
3. Identify the conditions that appear to cause organisms to produce specific metal-binding ligands, such as amphibactins in low-Fe/N waters and exceptionally strong Cu-binding ligands in upwelling regimes.
4. Determine the composition (organic versus inorganic) of cFe and other TEIs in surface waters and processes that regulate cFe composition, its bioavailability, and the fate of Fe within deep chlorophyll maxima.
5. Quantify the scavenging of Zn, Cu, and other particle-reactive TEIs from deep water and its impact on their isotopic composition.
6. Determine the extent to which TEIs are generally trapped on continental shelves and the processes responsible.
7. Identify the processes and conditions that generate the extensive deep plumes of Fe and Co observed at many continental margins and the extent to which these processes serve as sources of other TEIs.
8. Determine the amounts of the dissolved TEIs injected into the deep ocean by hydrothermal vents and those introduced at continental margins that survive until the water mass outcrops at the sea surface.
9. Quantify sources of TEIs from dust, margin sediments, submarine groundwater discharges, etc., by combining appropriate radionuclides and stable isotopes with trace metal distributions.
10. More generally, quantify benthic sources of TEIs, including those associated with nepheloid layers as well as the mobilization of TEIs during early sediment diagenesis.

This represents a partial list, to which additional targets will undoubtedly be added as more results become available, including those from GEOTRACES expeditions at high latitudes.

5.2. Contaminants

Although the GEOTRACES mission emphasizes natural biogeochemical cycles, the natural distributions of some of the TEIs under investigation have been perturbed by anthropogenic sources—most significantly, Pb. Maximum historical dPb concentrations measured in North Atlantic surface waters were more than an order of magnitude greater than concentrations currently in deep water (Boyle et al. 2014), which may be close to the preindustrial level in surface waters. GEOTRACES continues to document the long-term decline of Pb in the Atlantic following its elimination from motor fuels and other restrictions on its emission (Boyle et al. 2014, Bridgestock et al. 2016, Noble et al. 2015, Zurbrick et al. 2018). These findings demonstrate the success of policies enacted to reduce Pb contamination in the environment.

The surface-ocean inventory of Hg roughly tripled its preindustrial level due to anthropogenic emissions (Lamborg et al. 2014). As a neurotoxin that is bioaccumulated up the food chain, Hg is of special concern to environmental regulators. GEOTRACES studies have added new information about the concentration, speciation, and flux of Hg in the ocean (Bowman et al. 2015, 2016; Bratkic et al. 2016; Cossa et al. 2018a,b; Mason et al. 2017). For example, a hot spot of production

of methylated Hg, the form most subject to bioaccumulation, has been identified in the upper Arctic Ocean (Heimbürger et al. 2015). Future assessments of the impact of Hg contamination and, eventually, documentation of the improvements in response to emission controls will find a valuable resource in GEOTRACES data.

The growing use of Gd in medical procedures has led to its release into the environment. Although not yet detectable in the open ocean, an anthropogenic signal has been measured in coastal waters (Hatje et al. 2016, Pedreira et al. 2018). GEOTRACES data on rare earth elements will serve as a baseline to assess any future perturbation of the natural distribution of Gd or of any of the other rare earth elements experiencing growing use in industry. The anticipated growth of seabed mineral extraction may alter future trace element distributions in the deep sea (Lusty & Murton 2018). GEOTRACES data provide a baseline against which future changes can be assessed as well.

5.3. Chemical–Biological Coupling

Biological uptake and regeneration regulate the distributions of many TEIs in the ocean, so study of these processes constitutes a major effort toward completing the GEOTRACES mission. As a complement to these studies, an exploratory component was inserted within GEOTRACES, known as BioGEOTRACES, to encourage investigators to collect information, where possible, about the biological response to micronutrient availability.

Analysis of proteins collected along the GEOTRACES zonal section across the subtropical North Atlantic indicated that coastal *Synechococcus* strains have more strategies for acquiring and processing Fe than open ocean strains (Mackey et al. 2015). The distribution of nifH phylotypes along the same section identified significant differences in diazotroph communities on each side of the Atlantic (Ratten et al. 2015), a difference that was attributed to greater dust deposition in the east. In an exploratory study of the diversity of cyanobacteria along this section, Berube et al. (2018) reported data for 459 single-cell genomes of *Prochlorococcus* and 50 of *Synechococcus*, as well as for approximately 200 diverse other organisms. A complementary metagenomic study by Biller et al. (2018) reported data for 610 samples from three GEOTRACES cruises in the Atlantic and one in the Pacific. Synthesis of these results, including their comparison against measured distributions of micronutrients, will help target future studies of the sensitivity of marine ecosystems to micronutrient availability.

Other expeditions have used various strategies to assess micronutrient limitation. Shipboard incubations during a GEOTRACES cruise in the southeast Atlantic revealed locations and conditions under which phytoplankton growth was limited individually or sequentially by N, Fe, or Co (Browning et al. 2017). Declining diazotroph abundance eastward along a zonal GEOTRACES section in the southwest Pacific correlated with sources of dust, supporting the view that the supply of Fe by dust is a key factor regulating N fixation in the ocean (Ellwood et al. 2018). Along a meridional transect crossing the central equatorial Pacific, measurement of the abundances of multiple peptide biomarkers as indicators of stress in *Prochlorococcus* revealed overlapping regions of macronutrient stress, centered in the North Pacific subtropical gyre, and Fe stress within the equatorial upwelling system (Saito et al. 2014).

Results from these studies clearly indicate the potential for exploiting natural variability in macro- and micronutrient abundance to probe the responses of marine organisms to varying environmental conditions. Recognizing this opportunity to advance knowledge of chemical–biological coupling, an effort has been launched to organize a coordinated international approach to the problem. Now identified as Biogeoscapes (<http://www.biogeoscapes.org>), the group is exploring strategies that would build on the knowledge about the biogeochemical cycles of micronutrients

created by GEOTRACES. The design and development of other programs may similarly benefit by building on the experience and products of GEOTRACES.

DISCLOSURE STATEMENT

The author is not aware of any affiliations, memberships, funding, or financial holdings that might be perceived as affecting the objectivity of this review.

ACKNOWLEDGMENTS

Comments on earlier versions of this review by Mary-Elena Carr, Alessandro Tagliabue, Andy Bowie, Phoebe Lam, Catherine Jeandel, and Frankie Pavia, as well as by an anonymous referee, have improved the final product. Helpful guidance throughout the preparation of this review was provided by *Annual Review of Marine Science* Production Editor Jim Duncan. Frankie Pavia calculated the inventory ratios of excess dFe to excess ^3He in **Figure 6**. Preparation of this review was supported by the US National Science Foundation (NSF) through award OCE-1536294.

GEOTRACES has been successful because of funding for cruises and workshops from research councils in many nations. In addition, a wide variety of funders have contributed directly to the central organization of GEOTRACES, which has been critical to its operation as an international program. Of these, the NSF support managed through SCOR has been most substantial. Similarly, we thank all other such funders, including the UK Natural Environment Research Council, Ministry of Earth Science of India, Centre National de Recherche Scientifique, Observatoire Midi-Pyrénées, Universitat Autònoma de Barcelona, Kiel Excellence Cluster “The Future Ocean,” Swedish Museum of Natural History, University of Tokyo, University of British Columbia, Royal Netherlands Institute for Sea Research, GEOMAR-Helmholtz Centre for Ocean Research Kiel, and Alfred Wegener Institute. Management of GEOTRACES has benefited from oversight and direction provided by SCOR, especially from its executive director, Ed Urban. Don Rice at the NSF provided advice based on his experience with prior large ocean research programs that was invaluable in guiding GEOTRACES through its early days of planning and implementation.

LITERATURE CITED

- Abadie C, Lacan F, Radic A, Pradoux C, Poitras F. 2017. Iron isotopes reveal distinct dissolved iron sources and pathways in the intermediate versus deep Southern Ocean. *PNAS* 114:858–63
- Abouchami W, Galer SJG, de Baar HJW, Alderkamp AC, Middag R, et al. 2011. Modulation of the Southern Ocean cadmium isotope signature by ocean circulation and primary productivity. *Earth Planet. Sci. Lett.* 305:83–91
- Aguilar-Islas AM, Wu J, Rember R, Johansen AM, Shank LM. 2010. Dissolution of aerosol-derived iron in seawater: leach solution chemistry, aerosol type, and colloidal iron fraction. *Mar. Chem.* 120:25–33
- Anand SS, Rengarajan R, Shenoy D, Gauns M, Naqvi SWA. 2018. POC export fluxes in the Arabian Sea and the Bay of Bengal: a simultaneous $^{234}\text{Th}/^{238}\text{U}$ and $^{210}\text{Po}/^{210}\text{Pb}$ study. *Mar. Chem.* 198:70–87
- Anderson RF, Bacon MP, Brewer PG. 1983. Removal of ^{230}Th and ^{231}Pa at ocean margins. *Earth Planet. Sci. Lett.* 66:73–90
- Anderson RF, Cheng H, Edwards RL, Fleisher MQ, Hayes CT, et al. 2016. How well can we quantify dust deposition to the ocean? *Philos. Trans. R. Soc. A* 374:20150285
- Baars O, Abouchami W, Galer SJG, Boye M, Croot PL. 2014. Dissolved cadmium in the Southern Ocean: distribution, speciation, and relation to phosphate. *Limnol. Oceanogr.* 59:385–99
- Baars O, Croot PL. 2011. The speciation of dissolved zinc in the Atlantic sector of the Southern Ocean. *Deep-Sea Res. II* 58:2720–32

- Bacon MP, Anderson RF. 1982. Distribution of thorium isotopes between dissolved and particulate forms in the deep-sea. *J. Geophys. Res. Oceans* 87:2045–56
- Bacon MP, Spencer DW, Brewer PG. 1976. ^{210}Pb - ^{226}Ra and ^{210}Po - ^{210}Pb disequilibria in seawater and suspended particulate matter. *Earth Planet. Sci. Lett.* 32:277–96
- Baker AR, Landing WM, Bucciarelli E, Cheize M, Fietz S, et al. 2016. Trace element and isotope deposition across the air–sea interface: progress and research needs. *Philos. Trans. R. Soc. A* 374:20160190
- Basak C, Pahnke K, Frank M, Lamy F, Gersonde R. 2015. Neodymium isotopic characterization of Ross Sea Bottom Water and its advection through the southern South Pacific. *Earth Planet. Sci. Lett.* 419:211–21
- Behrens MK, Pahnke K, Schnetger B, Brumsack H-J. 2018. Sources and processes affecting the distribution of dissolved Nd isotopes and concentrations in the West Pacific. *Geochim. Cosmochim. Acta* 222:508–34
- Berube PM, Biller SJ, Hackl T, Hogle SL, Satinsky BM, et al. 2018. Single cell genomes of *Prochlorococcus*, *Synechococcus*, and sympatric microbes from diverse marine environments. *Sci. Data* 5:180154
- Biller SJ, Berube PM, Dooley K, Williams M, Satinsky BM, et al. 2018. Marine microbial metagenomes sampled across space and time. *Sci. Data* 5:180176
- Birchill AJ, Hartner NT, Kunde K, Siemering B, Daniels C, et al. 2019. The eastern extent of seasonal iron limitation in the high latitude North Atlantic Ocean. *Sci. Rep.* 9:1435
- Black EE, Buesseler KO, Pike SM, Lam PJ. 2018. ^{234}Th as a tracer of particulate export and remineralization in the southeastern tropical Pacific. *Mar. Chem.* 201:35–50
- Black EE, Lam PJ, Lee JM, Buesseler KO. 2019. Insights from the ^{238}U - ^{234}Th method into the coupling of biological export and the cycling of cadmium, cobalt, and manganese in the southeast Pacific Ocean. *Glob. Biogeochem. Cycles* 33:15–36
- Boiteau RM, Mende DR, Hawco NJ, McIlvin MR, Fitzsimmons JN, et al. 2016a. Siderophore-based microbial adaptations to iron scarcity across the eastern Pacific Ocean. *PNAS* 113:14237–42
- Boiteau RM, Till CP, Coale TH, Fitzsimmons JN, Bruland KW, Repeta DJ. 2019. Patterns of iron and siderophore distributions across the California Current System. *Limnol. Oceanogr.* 64:376–89
- Boiteau RM, Till CP, Ruacho A, Bundy RM, Hawco NJ, et al. 2016b. Structural characterization of natural nickel and copper binding ligands along the US GEOTRACES Eastern Pacific Zonal Transect. *Front. Mar. Sci.* 3:243
- Bourne HL, Bishop JKB, Lam PJ, Ohnemus DC. 2018. Global spatial and temporal variation of Cd:P in euphotic zone particulates. *Glob. Biogeochem. Cycles* 32:1123–41
- Bowie AR, van der Merwe P, Quéroué F, Trull T, Fourquez M, et al. 2015. Iron budgets for three distinct biogeochemical sites around the Kerguelen Archipelago (Southern Ocean) during the natural fertilisation study, KEOPS-2. *Biogeosciences* 12:4421–45
- Bowman KL, Hammerschmidt CR, Lamborg CH, Swarr GJ. 2015. Mercury in the North Atlantic Ocean: the U.S. GEOTRACES zonal and meridional sections. *Deep-Sea Res. II* 116:251–61
- Bowman KL, Hammerschmidt CR, Lamborg CH, Swarr GJ, Agather AM. 2016. Distribution of mercury species across a zonal section of the eastern tropical South Pacific Ocean (U.S. GEOTRACES GP16). *Mar. Chem.* 186:156–66
- Boyd PW, Ellwood MJ. 2010. The biogeochemical cycle of iron in the ocean. *Nat. Geosci.* 3:675–82
- Boyd PW, Ellwood MJ, Tagliabue A, Twining BS. 2017. Biotic and abiotic retention, recycling and remineralization of metals in the ocean. *Nat. Geosci.* 10:167–73
- Boyd PW, Ibanmni E, Sander SG, Hunter KA, Jackson GA. 2010. Remineralization of upper ocean particles: implications for iron biogeochemistry. *Limnol. Oceanogr.* 55:1271–88
- Boyd PW, Jickells T, Law CS, Blain S, Boyle EA, et al. 2007. Mesoscale iron enrichment experiments 1993–2005: synthesis and future directions. *Science* 315:612–17
- Boyd PW, Strzepek RF, Ellwood MJ, Hutchins DA, Nodder SD, et al. 2015. Why are biotic iron pools uniform across high- and low-iron pelagic ecosystems? *Glob. Biogeochem. Cycles* 29:1028–43
- Boyd PW, Tagliabue A. 2015. Using the L^* concept to explore controls on the relationship between paired ligand and dissolved iron concentrations in the ocean. *Mar. Chem.* 173:52–66
- Boye M, Nishioka J, Croot P, Laan P, Timmermans KR, et al. 2010. Significant portion of dissolved organic Fe complexes in fact is Fe colloids. *Mar. Chem.* 122:20–27

- Boyle EA, Edmond JM. 1975. Copper in surface waters south of New Zealand. *Nature* 253:107–9
- Boyle EA, Edmond JM, Sholkovitz ER. 1977. The mechanism of iron removal in estuaries. *Geochim. Cosmochim. Acta* 41:1313–24
- Boyle EA, Lee J-M, Echevoyen Y, Noble A, Moos S, et al. 2014. Anthropogenic lead emissions in the ocean: the evolving global experiment. *Oceanography* 27(1):69–75
- Boyle EA, Sclater F, Edmond JM. 1976. On the marine geochemistry of cadmium. *Nature* 263:42–44
- Bratkič A, Vahčić M, Kotnik J, Vazner KO, Begu E, et al. 2016. Mercury presence and speciation in the South Atlantic Ocean along the 40°S transect. *Glob. Biogeochem. Cycles* 30:105–19
- Bridgestock L, van de Flierdt T, Rehkämper M, Paul M, Middag R, et al. 2016. Return of naturally sourced Pb to Atlantic surface waters. *Nat. Commun.* 7:12921
- Broecker WS, Peng TH. 1982. *Tracers in the Sea*. Palisades, NY: Eldigio
- Browning TJ, Achterberg EP, Rapp I, Engel A, Bertrand EM, et al. 2017. Nutrient co-limitation at the boundary of an oceanic gyre. *Nature* 551:242–46
- Brunland KW. 1980. Oceanographic distributions of cadmium, zinc, nickel, and copper in the North Pacific. *Earth Planet. Sci. Lett.* 47:176–98
- Brunland KW. 1983. Trace elements in sea water. In *Chemical Oceanography*, ed. JP Riley, R Chester, pp. 157–220. London: Academic
- Brunland KW, Franks RP, Knauer GA, Martin JH. 1979. Sampling and analytical methods for the determination of copper, cadmium, zinc, and nickel at the nanogram per liter level in sea-water. *Anal. Chim. Acta* 105:233–45
- Brunland KW, Knauer GA, Martin JH. 1978a. Cadmium in northeast Pacific waters. *Limnol. Oceanogr.* 23:618–25
- Brunland KW, Knauer GA, Martin JH. 1978b. Zinc in northeast Pacific water. *Nature* 271:741–43
- Brunland KW, Middag R, Lohan MC. 2014. Controls of trace metals in seawater. In *Treatise on Geochemistry*, ed. KK Turekian, HD Holland, pp. 19–51. Oxford, UK: Elsevier. 2nd ed.
- Brzezinski MA, Jones JL. 2015. Coupling of the distribution of silicon isotopes to the meridional overturning circulation of the North Atlantic Ocean. *Deep-Sea Res. II* 116:79–88
- Buck CS, Aguilar-Islas A, Marsay C, Kadko D, Landing WM. 2019. Trace element concentrations, elemental ratios, and enrichment factors observed in aerosol samples collected during the US GEOTRACES Eastern Pacific Ocean Transect (GP16). *Chem. Geol.* 511:212–24
- Buck KN, Gerringa LJA, Rijkenberg MJA. 2016. An intercomparison of dissolved iron speciation at the Bermuda Atlantic Time-series Study (BATS) site: results from GEOTRACES crossover station A. *Front. Mar. Sci.* 3:262
- Buck KN, Lohan MC, Sander SG, Hassler C, Pižeta I. 2017. Editorial: organic ligands—a key control on trace metal biogeochemistry in the ocean. *Front. Mar. Sci.* 4:313
- Buck KN, Moffett J, Barbeau KA, Bundy RM, Kondo Y, Wu JF. 2012. The organic complexation of iron and copper: an intercomparison of competitive ligand exchange-adsorptive cathodic stripping voltammetry (CLE-ACSV) techniques. *Limnol. Oceanogr. Methods* 10:496–515
- Buck KN, Sedwick PN, Sohst B, Carlson CA. 2018. Organic complexation of iron in the eastern tropical South Pacific: results from US GEOTRACES Eastern Pacific Zonal Transect (GEOTRACES cruise GP16). *Mar. Chem.* 201:229–41
- Buck KN, Sohst B, Sedwick PN. 2015. The organic complexation of dissolved iron along the U.S. GEOTRACES (GA03) North Atlantic section. *Deep-Sea Res. II* 116:152–65
- Bundy RM, Jiang M, Carter M, Barbeau KA. 2016. Iron-binding ligands in the Southern California Current System: mechanistic studies. *Front. Mar. Sci.* 3:27
- Charette MA, Lam PJ, Lohan MC, Kwon EY, Hatje V, et al. 2016. Coastal ocean and shelf-sea biogeochemical cycling of trace elements and isotopes: lessons learned from GEOTRACES. *Philos. Trans. R. Soc. A* 374:20160076
- Charette MA, Morris PJ, Henderson PB, Moore WS. 2015. Radium isotope distributions during the US GEOTRACES North Atlantic cruises. *Mar. Chem.* 177:184–95
- Chase Z, Ellwood MJ, van de Flierdt T. 2018. Discovering the ocean's past through geochemistry. *Elements* 14:397–402

- Chever F, Bucciarelli E, Sarthou G, Speich S, Arhan M, et al. 2010. Physical speciation of iron in the Atlantic sector of the Southern Ocean along a transect from the subtropical domain to the Weddell Sea Gyre. *J. Geophys. Res. Oceans* 115:C10059
- Coale KH, Bruland KW. 1990. Spatial and temporal variability in copper complexation in the North Pacific. *Deep-Sea Res. A* 37:317–36
- Conway TM, John SG. 2014a. The biogeochemical cycling of zinc and zinc isotopes in the North Atlantic Ocean. *Glob. Biogeochem. Cycles* 28:1111–28
- Conway TM, John SG. 2014b. Quantification of dissolved iron sources to the North Atlantic Ocean. *Nature* 511:212–15
- Conway TM, John SG. 2015. The cycling of iron, zinc and cadmium in the North East Pacific Ocean – insights from stable isotopes. *Geochim. Cosmochim. Acta* 164:262–83
- Cossa D, Heimbürger LE, Pérez FF, García-Ibáñez MI, Sonke JE, et al. 2018a. Mercury distribution and transport in the North Atlantic Ocean along the GEOTRACES-GA01 transect. *Biogeosciences* 15:2309–23
- Cossa D, Heimbürger LE, Sonke JE, Planquette H, Lherminier P, et al. 2018b. Sources, cycling and transfer of mercury in the Labrador Sea (Geotraces-Geovide cruise). *Mar. Chem.* 198:64–69
- Craig H, Turekian KK. 1980. The GEOSECS program: 1976–1979. *Earth Planet. Sci. Lett.* 49:263–65
- Deng F, Henderson GM, Castrillejo M, Perez FF, Steinfeldt R. 2018. Evolution of ^{231}Pa and ^{230}Th in overflow waters of the North Atlantic. *Biogeosciences* 15:7299–313
- Deng F, Thomas AL, Rijkenberg MJA, Henderson GM. 2014. Controls on seawater ^{231}Pa , ^{230}Th and ^{232}Th concentrations along the flow paths of deep waters in the Southwest Atlantic. *Earth Planet. Sci. Lett.* 390:93–102
- Dulaquais G, Boye M, Middag R, Owens S, Puigcorbe V, et al. 2014a. Contrasting biogeochemical cycles of cobalt in the surface western Atlantic Ocean. *Glob. Biogeochem. Cycles* 28:2014GB004903
- Dulaquais G, Boye M, Rijkenberg MJA, Carton X. 2014b. Physical and remineralization processes govern the cobalt distribution in the deep western Atlantic Ocean. *Biogeosciences* 11:1561–80
- Dutay JC, Tagliabue A, Kriest I, van Hulst MMP. 2015. Modelling the role of marine particle on large scale ^{231}Pa , ^{230}Th , iron and aluminium distributions. *Prog. Oceanogr.* 133:66–72
- Ellwood MJ, Bowie AR, Baker A, Gault-Ringold M, Hassler C, et al. 2018. Insights into the biogeochemical cycling of iron, nitrate, and phosphate across a 5,300 km South Pacific zonal section (153°E–150°W). *Glob. Biogeochem. Cycles* 32:187–207
- Ellwood MJ, Hunter KA. 2000. The incorporation of zinc and iron into the frustule of the marine diatom *Thalassiosira pseudonana*. *Limnol. Oceanogr.* 45:1517–24
- Ellwood MJ, Hutchins DA, Lohan MC, Milne A, Nasemann P, et al. 2015. Iron stable isotopes track pelagic iron cycling during a subtropical phytoplankton bloom. *PNAS* 112:E15–20
- Fishwick MP, Sedwick PN, Lohan MC, Worsfold PJ, Buck KN, et al. 2014. The impact of changing surface ocean conditions on the dissolution of aerosol iron. *Glob. Biogeochem. Cycles* 28:1235–50
- Fishwick MP, Ussher SJ, Sedwick PN, Lohan MC, Worsfold PJ, et al. 2018. Impact of surface ocean conditions and aerosol provenance on the dissolution of aerosol manganese, cobalt, nickel and lead in seawater. *Mar. Chem.* 198:28–43
- Fitzsimmons JN, Boyle EA. 2014. Both soluble and colloidal iron phases control dissolved iron variability in the tropical North Atlantic Ocean. *Geochim. Cosmochim. Acta* 125:539–50
- Fitzsimmons JN, Bundy RM, Al-Subiaí SN, Barbeau KA, Boyle EA. 2015a. The composition of dissolved iron in the dusty surface ocean: an exploration using size-fractionated iron-binding ligands. *Mar. Chem.* 173:125–35
- Fitzsimmons JN, Carrasco GG, Wu J, Roshan S, Hatta M, et al. 2015b. Partitioning of dissolved iron and iron isotopes into soluble and colloidal phases along the GA03 GEOTRACES North Atlantic Transect. *Deep-Sea Res. II* 116:130–51
- Fitzsimmons JN, Hayes CT, Al-Subiaí SN, Zhang R, Morton PL, et al. 2015c. Daily to decadal variability of size-fractionated iron and iron-binding ligands at the Hawaii Ocean Time-series Station ALOHA. *Geochim. Cosmochim. Acta* 171:303–24

- Fitzsimmons JN, John SG, Marsay CM, Hoffinan CL, Nicholas SL, et al. 2017. Iron persistence in a distal hydrothermal plume supported by dissolved-particulate exchange. *Nat. Geosci.* 10:195–201
- Frants M, Holzer M, DeVries T, Matear R. 2016. Constraints on the global marine iron cycle from a simple inverse model. *J. Geophys. Res. Biogeosci.* 121:28–51
- Garcia-Solsona E, Jeandel C, Labatut M, Lacan F, Vance D, et al. 2014. Rare earth elements and Nd isotopes tracing water mass mixing and particle-seawater interactions in the SE Atlantic. *Geochim. Cosmochim. Acta* 125:351–72
- Gardner WD, Richardson MJ, Mishonov AV. 2018a. Global assessment of benthic nepheloid layers and linkage with upper ocean dynamics. *Earth Planet. Sci. Lett.* 482:126–34
- Gardner WD, Richardson MJ, Mishonov AV, Biscaye PE. 2018b. Global comparison of benthic nepheloid layers based on 52 years of nephelometer and transmissometer measurements. *Prog. Oceanogr.* 168:100–11
- Geibert W. 2018. Processes that regulate trace element distribution in the ocean. *Elements* 14:391–96
- GEOTRACES Plan. Group. 2006. *GEOTRACES Science Plan*. Baltimore, MD: Sci. Comm. Ocean. Res.
- German CR, Casciotti KA, Dutay JC, Heimbürger LE, Jenkins WJ, et al. 2016. Hydrothermal impacts on trace element and isotope ocean biogeochemistry. *Philos. Trans. R. Soc. A* 374:20160035
- German CR, Fleer AP, Bacon MP, Edmond JM. 1991. Hydrothermal scavenging at the Mid-Atlantic Ridge: radionuclide distributions. *Earth Planet. Sci. Lett.* 105:170–81
- Gerringa LJA, Rijkenberg MJA, Schoemann V, Laan P, de Baar HJW. 2015. Organic complexation of iron in the West Atlantic Ocean. *Mar. Chem.* 177:434–46
- Gerringa LJA, Slagter HA, Bown J, van Haren H, Laan P, et al. 2017. Dissolved Fe and Fe-binding organic ligands in the Mediterranean Sea – GEOTRACES G04. *Mar. Chem.* 194:100–13
- Gledhill M, Buck K. 2012. The organic complexation of iron in the marine environment: a review. *Front. Microbiol.* 3:69
- Grasse P, Bosse L, Hathorne EC, Böning P, Pahnke K, Frank M. 2017. Short-term variability of dissolved rare earth elements and neodymium isotopes in the entire water column of the Panama Basin. *Earth Planet. Sci. Lett.* 475:242–53
- Hatje V, Bruland KW, Flegal AR. 2016. Increases in anthropogenic gadolinium anomalies and rare earth element concentrations in San Francisco Bay over a 20 year record. *Environ. Sci. Technol.* 50:4159–68
- Hatta M, Measures CI, Wu J, Roshan S, Fitzsimmons JN, et al. 2015. An overview of dissolved Fe and Mn distributions during the 2010–2011 U.S. GEOTRACES North Atlantic cruises: GEOTRACES GA03. *Deep-Sea Res. II* 116:117–29
- Hawco NJ, Lam PJ, Lee J-M, Ohnemus DC, Noble AE, et al. 2018. Cobalt scavenging in the mesopelagic ocean and its influence on global mass balance: synthesizing water column and sedimentary fluxes. *Mar. Chem.* 201:151–66
- Hawco NJ, Ohnemus DC, Resing JA, Twining BS, Saito MA. 2016. A dissolved cobalt plume in the oxygen minimum zone of the eastern tropical South Pacific. *Biogeosciences* 13:5697–717
- Hayes CT, Anderson RF, Cheng H, Conway TM, Edwards RL, et al. 2018a. Replacement times of a spectrum of elements in the North Atlantic based on thorium supply. *Glob. Biogeochem. Cycles* 32:1294–311
- Hayes CT, Anderson RF, Fleisher MQ, Huang K-F, Robinson LF, et al. 2015a. ²³⁰Th and ²³¹Pa on GEOTRACES GA03, the U.S. GEOTRACES North Atlantic Transect, and implications for modern and paleoceanographic chemical fluxes. *Deep-Sea Res. II* 116:29–41
- Hayes CT, Anderson RF, Fleisher MQ, Serno S, Winckler G, Gersonde R. 2013. Quantifying lithogenic inputs to the North Pacific Ocean using the long-lived thorium isotopes. *Earth Planet. Sci. Lett.* 383:16–25
- Hayes CT, Black EE, Anderson RF, Baskaran M, Buesseler KO, et al. 2018b. Flux of particulate elements in the North Atlantic Ocean constrained by multiple radionuclides. *Glob. Biogeochem. Cycles* 32:1738–58
- Hayes CT, Fitzsimmons JN, Boyle EA, McGee D, Anderson RF, et al. 2015b. Thorium isotopes tracing the iron cycle at the Hawaii Ocean Time-series Station ALOHA. *Geochim. Cosmochim. Acta* 169:1–16
- Heimbürger L-E, Sonke JE, Cossa D, Point D, Lagane C, et al. 2015. Shallow methylmercury production in the marginal sea ice zone of the central Arctic Ocean. *Sci. Rep.* 5:10318

- Heller MI, Croot PL. 2015. Copper speciation and distribution in the Atlantic sector of the Southern Ocean. *Mar. Chem.* 173:253–68
- Heller MI, Lam PJ, Moffett JW, Till CP, Lee J-M, et al. 2017. Accumulation of Fe oxyhydroxides in the Peruvian oxygen deficient zone implies non-oxygen dependent Fe oxidation. *Geochim. Cosmochim. Acta* 211:174–93
- Henderson GM. 2002. New oceanic proxies for paleoclimate. *Earth Planet. Sci. Lett.* 203:1–13
- Henderson GM, Anderson RF. 2003. The U-series toolbox for paleoceanography. *Rev. Mineral. Geochem.* 52:493–529
- Holzer M, Brzezinski MA. 2015. Controls on the silicon isotope distribution in the ocean: new diagnostics from a data-constrained model. *Glob. Biogeochem. Cycles* 29:267–87
- Horner TJ, Kinsley CW, Nielsen SG. 2015. Barium-isotopic fractionation in seawater mediated by barite cycling and oceanic circulation. *Earth Planet. Sci. Lett.* 430:511–22
- Hsieh Y-T, Henderson GM. 2017. Barium stable isotopes in the global ocean: tracer of Ba inputs and utilization. *Earth Planet. Sci. Lett.* 473:269–78
- Hsieh Y-T, Henderson GM, Thomas AL. 2011. Combining seawater ^{232}Th and ^{230}Th concentrations to determine dust fluxes to the surface ocean. *Earth Planet. Sci. Lett.* 312:280–90
- Hutchins DA, Boyd PW. 2016. Marine phytoplankton and the changing ocean iron cycle. *Nat. Clim. Change* 6:1072–79
- Jacquot JE, Moffett JW. 2015. Copper distribution and speciation across the international GEOTRACES section GA03. *Deep-Sea Res. II* 116:187–207
- Janssen DJ, Abouchami W, Galer SJG, Purdon KB, Cullen JT. 2019. Particulate cadmium stable isotopes in the subarctic northeast Pacific reveal dynamic Cd cycling and a new isotopically light Cd sink. *Earth Planet. Sci. Lett.* 515:67–78
- Janssen DJ, Conway TM, John SG, Christian JR, Kramer DI, et al. 2014. Undocumented water column sink for cadmium in open ocean oxygen-deficient zones. *PNAS* 111:6888–93
- Jeandel C. 2016. Overview of the mechanisms that could explain the ‘boundary exchange’ at the land-ocean contact. *Philos. Trans. R. Soc. A* 374:20150287
- Jeandel C, Vance D. 2018. New tools, new discoveries in marine geochemistry. *Elements* 14:379–84
- Jenkins WJ, Lott DE, German CR, Cahill KL, Goudreau J, Longworth B. 2018. The deep distributions of helium isotopes, radiocarbon, and noble gases along the U.S. GEOTRACES East Pacific Zonal Transect (GP16). *Mar. Chem.* 201:167–82
- Jickells TD, An ZS, Andersen KK, Baker AR, Bergametti G, et al. 2005. Global iron connections between desert dust, ocean biogeochemistry, and climate. *Science* 308:67–71
- Jickells TD, Baker AR, Chance R. 2016. Atmospheric transport of trace elements and nutrients to the oceans. *Philos. Trans. R. Soc. A* 374:20150286
- Jickells TD, Moore CM. 2015. The importance of atmospheric deposition for ocean productivity. *Annu. Rev. Ecol. Evol. Syst.* 46:481–501
- John SG, Conway TM. 2014. A role for scavenging in the marine biogeochemical cycling of zinc and zinc isotopes. *Earth Planet. Sci. Lett.* 394:159–67
- John SG, Helgoe J, Townsend E, Weber T, DeVries T, et al. 2018. Biogeochemical cycling of Fe and Fe stable isotopes in the eastern tropical South Pacific. *Mar. Chem.* 201:66–76
- Kadko D, Aguilar-Islas A, Bolt C, Buck CS, Fitzsimmons JN, et al. 2019. The residence times of trace elements determined in the surface Arctic Ocean during the 2015 US Arctic GEOTRACES expedition. *Mar. Chem.* 208:56–69
- Kadko D, Landing WM, Shelley RU. 2015. A novel tracer technique to quantify the atmospheric flux of trace elements to remote ocean regions. *J. Geophys. Res. Oceans* 120:848–58
- Kim T, Obata H, Kondo Y, Ogawa H, Gamo T. 2015. Distribution and speciation of dissolved zinc in the western North Pacific and its adjacent seas. *Mar. Chem.* 173:330–41
- Kim T, Obata H, Nishioka J, Gamo T. 2017. Distribution of dissolved zinc in the western and central subarctic North Pacific. *Glob. Biogeochem. Cycles* 31:1454–68
- Kipp LE, Sanial V, Henderson PB, van Beek P, Reyss J-L, et al. 2018. Radium isotopes as tracers of hydrothermal inputs and neutrally buoyant plume dynamics in the deep ocean. *Mar. Chem.* 201:51–65

- Klunder MB, Laan P, Middag R, de Baar HJW, Ooijen JV. 2011. Dissolved iron in the Southern Ocean (Atlantic sector). *Deep-Sea Res. II* 58:2678–94
- Labatut M, Lacan F, Pradoux C, Chmeleff J, Radic A, et al. 2014. Iron sources and dissolved-particulate interactions in the seawater of the Western Equatorial Pacific, iron isotope perspectives. *Glob. Biogeochem. Cycles* 28:1044–65
- Lam PJ, Ohnemus DC, Auro ME. 2015. Size-fractionated major particle composition and concentrations from the US GEOTRACES North Atlantic Zonal Transect. *Deep-Sea Res. II* 116:303–20
- Lambelet M, van de Flierdt T, Butler ECV, Bowie AR, Rintoul SR, et al. 2018. The neodymium isotope fingerprint of Adélie Coast Bottom Water. *Geophys. Res. Lett.* 45:11247–56
- Lambelet M, van de Flierdt T, Crockett K, Rehkämper M, Kreissig K, et al. 2016. Neodymium isotopic composition and concentration in the western North Atlantic Ocean: results from the GEOTRACES GA02 section. *Geochim. Cosmochim. Acta* 177:1–29
- Lamborg C, Bowman K, Hammerschmidt C, Gilmour C, Munson K, et al. 2014. Mercury in the Anthropocene ocean. *Oceanography* 27(1):76–87
- Lee J-M, Heller MI, Lam PJ. 2018. Size distribution of particulate trace elements in the U.S. GEOTRACES Eastern Pacific Zonal Transect (GP16). *Mar. Chem.* 201:108–23
- Lemaître N, Planchon F, Planquette H, Dehairs F, Fonseca-Batista D, et al. 2018. High variability of particulate organic carbon export along the North Atlantic GEOTRACES section GA01 as deduced from ^{234}Th fluxes. *Biogeosciences* 15:6417–37
- Lerner P, Marchal O, Lam PJ, Buesseler K, Charette M. 2017. Kinetics of thorium and particle cycling along the U.S. GEOTRACES North Atlantic Transect. *Deep-Sea Res. I* 125:106–28
- Lerner P, Marchal O, Lam PJ, Solow A. 2018. Effects of particle composition on thorium scavenging in the North Atlantic. *Geochim. Cosmochim. Acta* 233:115–34
- Lis H, Shaked Y, Kranzler C, Keren N, Morel FMM. 2015. Iron bioavailability to phytoplankton: an empirical approach. *ISME J.* 9:1003–13
- Lohan MC, Buck KN, Sander SG. 2015. Organic ligands—a key control on trace metal biogeochemistry in the oceans. *Mar. Chem.* 173:1–2
- Lohan MC, Tagliabue A. 2018. Oceanic micronutrients: trace metals that are essential for marine life. *Elements* 14:385–90
- Lusty PAJ, Murton BJ. 2018. Deep-ocean mineral deposits: metal resources and windows into earth processes. *Elements* 14:301–6
- Mackey KRM, Post AF, McIlvin MR, Cutter GA, John SG, Saito MA. 2015. Divergent responses of Atlantic coastal and oceanic *Synechococcus* to iron limitation. *PNAS* 112:9944–49
- Marconi D, Sigman DM, Casciotti KL, Campbell EC, Weigand MA, et al. 2017. Tropical dominance of N_2 fixation in the North Atlantic Ocean. *Glob. Biogeochem. Cycles* 31:1608–23
- Marconi D, Weigand MA, Rafter PA, McIlvin MR, Forbes M, et al. 2015. Nitrate isotope distributions on the US GEOTRACES North Atlantic cross-basin section: signals of polar nitrate sources and low latitude nitrogen cycling. *Mar. Chem.* 177:143–56
- Marconi D, Weigand MA, Sigman DM. 2019. Nitrate isotopic gradients in the North Atlantic Ocean and the nitrogen isotopic composition of sinking organic matter. *Deep-Sea Res. I* 145:109–24
- Marsay CM, Lam PJ, Heller MI, Lee J-M, John SG. 2018. Distribution and isotopic signature of ligand-leachable particulate iron along the GEOTRACES GP16 East Pacific Zonal Transect. *Mar. Chem.* 201:198–211
- Martin TS, Primeau F, Casciotti KL. 2019. Modeling oceanic nitrate and nitrite concentrations and isotopes using a 3-D inverse N cycle model. *Biogeosciences* 16:347–67
- Mason RP, Hammerschmidt CR, Lamborg CH, Bowman KL, Swarr GJ, Shelley RU. 2017. The air-sea exchange of mercury in the low latitude Pacific and Atlantic Oceans. *Deep-Sea Res. I* 122:17–28
- Mawji E, Gledhill M, Milton JA, Tarran GA, Ussher S, et al. 2008. Hydroxamate siderophores: occurrence and importance in the Atlantic Ocean. *Environ. Sci. Technol.* 42:8675–80
- Measures C, Hatta M, Fitzsimmons J, Morton P. 2015. Dissolved Al in the zonal N Atlantic section of the US GEOTRACES 2010/2011 cruises and the importance of hydrothermal inputs. *Deep-Sea Res. II* 116:176–86

- Measures CI, Landing WM, Brown MT, Buck CS. 2008. High-resolution Al and Fe data from the Atlantic Ocean CLIVAR-CO₂ repeat hydrography A16N transect: extensive linkages between atmospheric dust and upper ocean geochemistry. *Glob. Biogeochem. Cycles* 22:GB1005
- Middag R, de Baar HJW, Bruland KW. 2019. The relationships between dissolved zinc and major nutrients phosphate and silicate along the GEOTRACES GA02 transect in the West Atlantic Ocean. *Glob. Biogeochem. Cycles* 33:63–84
- Middag R, van Heuven SMAC, Bruland KW, de Baar HJW. 2018. The relationship between cadmium and phosphate in the Atlantic Ocean unravelled. *Earth Planet. Sci. Lett.* 492:79–88
- Middag R, van Hulten MMP, Van Aken HM, Rijkenberg MJA, Gerringa LJA, et al. 2015. Dissolved aluminium in the ocean conveyor of the West Atlantic Ocean: effects of the biological cycle, scavenging, sediment resuspension and hydrography. *Mar. Chem.* 177:69–86
- Middag R, van Slooten C, de Baar HJW, Laan P. 2011. Dissolved aluminium in the Southern Ocean. *Deep-Sea Res. II* 58:2647–60
- Milne A, Schlosser C, Wake BD, Achterberg EP, Chance R, et al. 2017. Particulate phases are key in controlling dissolved iron concentrations in the (sub)tropical North Atlantic. *Geophys. Res. Lett.* 44:2377–87
- Moore CM. 2016. Diagnosing oceanic nutrient deficiency. *Philos. Trans. R. Soc. A* 374:20150290
- Moore CM, Mills MM, Achterberg EP, Geider RJ, LaRoche J, et al. 2009. Large-scale distribution of Atlantic nitrogen fixation controlled by iron availability. *Nat. Geosci.* 2:867–71
- Moore CM, Mills MM, Arrigo KR, Berman-Frank I, Bopp L, et al. 2013. Processes and patterns of oceanic nutrient limitation. *Nat. Geosci.* 6:701–10
- Moos SB, Boyle EA. 2019. Determination of accurate and precise chromium isotope ratios in seawater samples by MC-ICP-MS illustrated by analysis of SAFe Station in the North Pacific Ocean. *Chem. Geol.* 511:481–93
- Morel FMM, Price NM. 2003. The biogeochemical cycles of trace metals in the oceans. *Science* 300:944–47
- Niedermiller J, Baskaran M. 2019. Comparison of the scavenging intensity, remineralization and residence time of ²¹⁰Po and ²¹⁰Pb at key zones (biotic, sediment-water and hydrothermal) along the East Pacific GEOTRACES transect. *J. Environ. Radioact.* 198:165–88
- Nishioka J, Obata H. 2017. Dissolved iron distribution in the western and central subarctic Pacific: HNLC water formation and biogeochemical processes. *Limnol. Oceanogr.* 62:2004–22
- Noble AE, Echegoyen-Sanz Y, Boyle EA, Ohnemus DC, Lam PJ, et al. 2015. Dynamic variability of dissolved Pb and Pb isotope composition from the U.S. North Atlantic GEOTRACES transect. *Deep-Sea Res. II* 116:208–25
- Noble AE, Lamborg CH, Ohnemus DC, Lam PJ, Goepfert TJ, et al. 2012. Basin-scale inputs of cobalt, iron, and manganese from the Benguela-Angola front to the South Atlantic Ocean. *Limnol. Oceanogr.* 57:989–1010
- Noble AE, Ohnemus DC, Hawco NJ, Lam PJ, Saito MA. 2017. Coastal sources, sinks and strong organic complexation of dissolved cobalt within the US North Atlantic GEOTRACES transect GA03. *Biogeosciences* 14:2715–39
- Ohnemus DC, Rauschenberg S, Cutter GA, Fitzsimmons JN, Sherrell RM, Twining BS. 2017. Elevated trace metal content of prokaryotic communities associated with marine oxygen deficient zones. *Limnol. Oceanogr.* 62:3–25
- Owens SA, Pike S, Buesseler KO. 2015. Thorium-234 as a tracer of particle dynamics and upper ocean export in the Atlantic Ocean. *Deep-Sea Res. II* 116:42–59
- Pavia FJ, Anderson RF, Black EE, Kipp LE, Vivancos SM, et al. 2019. Timescales of hydrothermal scavenging in the South Pacific Ocean from ²³⁴Th, ²³⁰Th, and ²²⁸Th. *Earth Planet. Sci. Lett.* 506:146–56
- Pavia FJ, Anderson RF, Lam PJ, Cael BB, Vivancos SM, et al. 2019. Shallow particulate organic carbon regeneration in the South Pacific Ocean. *PNAS* 116:9753–58
- Pavia FJ, Anderson RF, Vivancos S, Fleisher MQ, Lam PJ, et al. 2018. Intense hydrothermal scavenging of ²³⁰Th and ²³¹Pa in the deep Southeast Pacific. *Mar. Chem.* 201:212–28
- Pedreira RMA, Pahnke K, Böning P, Hatje V. 2018. Tracking hospital effluent-derived gadolinium in Atlantic coastal waters off Brazil. *Water Res.* 145:62–72

- Peters BD, Lam PJ, Casciotti KL. 2018. Nitrogen and oxygen isotope measurements of nitrate along the US GEOTRACES Eastern Pacific Zonal Transect (GP16) yield insights into nitrate supply, remineralization, and water mass transport. *Mar. Chem.* 201:137–50
- Pham ALD, Ito T. 2018. Formation and maintenance of the GEOTRACES subsurface-dissolved iron maxima in an ocean biogeochemistry model. *Glob. Biogeochem. Cycles* 32:932–53
- Planchon F, Ballas D, Cavagna AJ, Bowie AR, Davies D, et al. 2015. Carbon export in the naturally iron-fertilized Kerguelen area of the Southern Ocean based on the ^{234}Th approach. *Biogeosciences* 12:3831–48
- Puigcorb  V, Roca-Mart  M, Masqu  P, Benitez-Nelson CR, Rutgers van der Loeff M, et al. 2017. Particulate organic carbon export across the Antarctic Circumpolar Current at 10 E: differences between north and south of the Antarctic Polar Front. *Deep-Sea Res. II* 138:86–101
- Quay P, Cullen J, Landing W, Morton P. 2015. Processes controlling the distributions of Cd and PO_4 in the ocean. *Glob. Biogeochem. Cycles* 29:830–41
- Quay P, Wu J. 2015. Impact of end-member mixing on depth distributions of $\delta^{13}\text{C}$, cadmium and nutrients in the N. Atlantic Ocean. *Deep-Sea Res. II* 116:107–16
- Ratten J-M, LaRoche J, Desai DK, Shelley RU, Landing WM, et al. 2015. Sources of iron and phosphate affect the distribution of diazotrophs in the North Atlantic. *Deep-Sea Res. II* 116:332–41
- Rempfer J, Stocker TF, Joos F, Lippold J, Jaccard SL. 2017. New insights into cycling of ^{231}Pa and ^{230}Th in the Atlantic Ocean. *Earth Planet. Sci. Lett.* 468:27–37
- Resing JA, Sedwick PN, German CR, Jenkins WJ, Moffett JW, et al. 2015. Basin-scale transport of hydrothermal dissolved metals across the South Pacific Ocean. *Nature* 523:200–3
- Revels BN, Ohnemus DC, Lam PJ, Conway TM, John SG. 2015. The isotopic signature and distribution of particulate iron in the North Atlantic Ocean. *Deep-Sea Res. II* 116:321–31
- Rigaud S, Stewart G, Baskaran M, Marsan D, Church T. 2015. ^{210}Po and ^{210}Pb distribution, dissolved-particulate exchange rates, and particulate export along the North Atlantic US GEOTRACES GA03 section. *Deep-Sea Res. II* 116:60–78
- Rijkenberg MJA, Middag R, Laan P, Gerringa LJA, van Aken HM, et al. 2014. The distribution of dissolved iron in the West Atlantic Ocean. *PLOS ONE* 9:e101323
- Roshan S, DeVries T, Wu J, Chen G. 2018. The internal cycling of zinc in the ocean. *Glob. Biogeochem. Cycles* 32:1833–49
- Roshan S, Wu J. 2015a. Cadmium regeneration within the North Atlantic. *Glob. Biogeochem. Cycles* 29:2082–94
- Roshan S, Wu J. 2015b. The distribution of dissolved copper in the tropical-subtropical north Atlantic across the GEOTRACES GA03 transect. *Mar. Chem.* 176:189–98
- Roshan S, Wu J. 2015c. Water mass mixing: the dominant control on the zinc distribution in the North Atlantic Ocean. *Glob. Biogeochem. Cycles* 29:1060–74
- Roshan S, Wu J, DeVries T. 2017. Controls on the cadmium-phosphate relationship in the tropical South Pacific. *Glob. Biogeochem. Cycles* 31:1516–27
- Roshan S, Wu J, Jenkins WJ. 2016. Long-range transport of hydrothermal dissolved Zn in the tropical South Pacific. *Mar. Chem.* 183:25–32
- Rousseau TCC, Sonke JE, Chmieleff J, van Beek P, Souhaut M, et al. 2015. Rapid neodymium release to marine waters from lithogenic sediments in the Amazon estuary. *Nat. Commun.* 6:7592
- Saito MA, McIlvin MR, Moran DM, Goepfert TJ, DiTullio GR, et al. 2014. Multiple nutrient stresses at intersecting Pacific Ocean biomes detected by protein biomarkers. *Science* 345:1173–77
- Saito MA, Noble AE, Hawco N, Twining BS, Ohnemus DC, et al. 2017. The acceleration of dissolved cobalt’s ecological stoichiometry due to biological uptake, remineralization, and scavenging in the Atlantic Ocean. *Biogeosciences* 14:4637–62
- Saito MA, Rocap G, Moffett JW. 2005. Production of cobalt binding ligands in a *Synechococcus* feature at the Costa Rica upwelling dome. *Limnol. Oceanogr.* 50:279–90
- Samanta M, Ellwood MJ, Sinoir M, Hassler CS. 2017. Dissolved zinc isotope cycling in the Tasman Sea, SW Pacific Ocean. *Mar. Chem.* 192:1–12

- Samanta S, Dalai TK. 2016. Dissolved and particulate barium in the Ganga (Hooghly) River estuary, India: solute-particle interactions and the enhanced dissolved flux to the oceans. *Geochim. Cosmochim. Acta* 195:1–28
- Samanta S, Dalai TK. 2018. Massive production of heavy metals in the Ganga (Hooghly) River estuary, India: global importance of solute-particle interaction and enhanced metal fluxes to the oceans. *Geochim. Cosmochim. Acta* 228:243–58
- Sanial V, Kipp LE, Henderson PB, van Beek P, Reyss JL, et al. 2018. Radium-228 as a tracer of dissolved trace element inputs from the Peruvian continental margin. *Mar. Chem.* 201:20–34
- Sarmiento JL, Gruber N, Brzezinski MA, Dunne JP. 2004. High-latitude controls of thermocline nutrients and low latitude biological productivity. *Nature* 427:56–60
- Scheiderich K, Amini M, Holmden C, Francois R. 2015. Global variability of chromium isotopes in seawater demonstrated by Pacific, Atlantic, and Arctic Ocean samples. *Earth Planet. Sci. Lett.* 423:87–97
- Schlitzer R, Anderson RF, Masferrer-Dodas E, Lohan M, Geibert W, et al. 2018. The GEOTRACES Intermediate Data Product 2017. *Chem. Geol.* 493:210–23
- Shelley RU, Landing WM, Ussher SJ, Planquette H, Sarthou G. 2018. Regional trends in the fractional solubility of Fe and other metals from North Atlantic aerosols (GEOTRACES cruises GA01 and GA03) following a two-stage leach. *Biogeosciences* 15:2271–88
- Shelley RU, Morton PL, Landing WM. 2015. Elemental ratios and enrichment factors in aerosols from the US-GEOTRACES North Atlantic transects. *Deep-Sea Res. II* 116:262–72
- Shelley RU, Roca-Martí M, Castrillejo M, Masqué P, Landing WM, et al. 2017. Quantification of trace element atmospheric deposition fluxes to the Atlantic Ocean (>40°N; GEOVIDE, GEOTRACES GA01) during spring 2014. *Deep-Sea Res. I* 119:34–49
- Sholkovitz ER, Sedwick PN, Church TM, Baker AR, Powell CF. 2012. Fractional solubility of aerosol iron: synthesis of a global-scale data set. *Geochim. Cosmochim. Acta* 89:173–89
- Sigman DM, Boyle EA. 2000. Glacial/interglacial variations in atmospheric carbon dioxide. *Nature* 407:859–69
- Singh SP, Singh SK, Bhushan R. 2013. Internal cycling of dissolved barium in water column of the Bay of Bengal. *Mar. Chem.* 154:12–23
- Singh SP, Singh SK, Goswami V, Bhushan R, Rai VK. 2012. Spatial distribution of dissolved neodymium and ϵ_{Nd} in the Bay of Bengal: role of particulate matter and mixing of water masses. *Geochim. Cosmochim. Acta* 94:38–56
- Sinoir M, Ellwood MJ, Butler ECV, Bowie AR, Mongin M, Hassler CS. 2016. Zinc cycling in the Tasman Sea: distribution, speciation and relation to phytoplankton community. *Mar. Chem.* 182:25–37
- Stichel T, Hartman AE, Duggan B, Goldstein SL, Scher H, Pahnke K. 2015. Separating biogeochemical cycling of neodymium from water mass mixing in the Eastern North Atlantic. *Earth Planet. Sci. Lett.* 412:245–60
- Stichel T, Pahnke K, Duggan B, Goldstein SL, Hartman AE, et al. 2018. TAG plume: revisiting the hydrothermal neodymium contribution to seawater. *Front. Mar. Sci.* 5:96
- Sunda WG. 1997. Control of dissolved iron concentrations in the world ocean: a comment. *Mar. Chem.* 57:169–72
- Sunda WG. 2012. Feedback interactions between trace metal nutrients and phytoplankton in the ocean. *Front. Microbiol.* 3:204
- Tachikawa K, Arsouze T, Bayon G, Bory A, Colin C, et al. 2017. The large-scale evolution of neodymium isotopic composition in the global modern and Holocene ocean revealed from seawater and archive data. *Chem. Geol.* 457:131–48
- Tagliabue A, Aumont O, Bopp L. 2014a. The impact of different external sources of iron on the global carbon cycle. *Geophys. Res. Lett.* 41:920–26
- Tagliabue A, Aumont O, DeAth R, Dunne JP, Dutkiewicz S, et al. 2016. How well do global ocean biogeochemistry models simulate dissolved iron distributions? *Glob. Biogeochem. Cycles* 30:149–74
- Tagliabue A, Bowie AR, Boyd PW, Buck KN, Johnson KS, Saito MA. 2017. The integral role of iron in ocean biogeochemistry. *Nature* 543:51–59

- Tagliabue A, Hawco NJ, Bundy RM, Landing WM, Milne A, et al. 2018. The role of external inputs and internal cycling in shaping the global ocean cobalt distribution: insights from the first cobalt biogeochemical model. *Glob. Biogeochem. Cycles* 32:594–616
- Tagliabue A, Resing J. 2016. Impact of hydrothermalism on the ocean iron cycle. *Philos. Trans. R. Soc. A* 374:20150291
- Tagliabue A, Williams RG, Rogan N, Achterberg EP, Boyd PW. 2014b. A ventilation-based framework to explain the regeneration-scavenging balance of iron in the ocean. *Geophys. Res. Lett.* 41:7227–36
- Thompson CM, Ellwood MJ, Sander SG. 2014. Dissolved copper speciation in the Tasman Sea, SW Pacific Ocean. *Mar. Chem.* 164:84–94
- Tuerena RE, Ganeshram RS, Geibert W, Fallick AE, Dougans J, et al. 2015. Nutrient cycling in the Atlantic basin: the evolution of nitrate isotope signatures in water masses. *Glob. Biogeochem. Cycles* 29:1830–44
- Twining BS, Baines SB. 2013. The trace metal composition of marine phytoplankton. *Annu. Rev. Mar. Sci.* 5:191–215
- Twining BS, Nodder SD, King AL, Hutchins DA, LeClerc GR, et al. 2014. Differential remineralization of major and trace elements in sinking diatoms. *Limnol. Oceanogr.* 59:689–704
- Twining BS, Rauschenberg S, Morton PL, Vogt S. 2015. Metal contents of phytoplankton and labile particulate material in the North Atlantic Ocean. *Prog. Oceanogr.* 137:261–83
- van Hulst MMP, Dutay JC, Roy-Barman M. 2018. A global scavenging and circulation ocean model of thorium-230 and protactinium-231 with improved particle dynamics (NEMO-ProThorP 0.1). *Geosci. Model. Dev.* 11:3537–56
- van Hulst MMP, Sterl A, Middag R, de Baar HJW, Gehlen M, et al. 2014. On the effects of circulation, sediment resuspension and biological incorporation by diatoms in an ocean model of aluminium. *Biogeosciences* 11:3757–79
- van Hulst MMP, Sterl A, Tagliabue A, Dutay JC, Gehlen M, et al. 2013. Aluminium in an ocean general circulation model compared with the West Atlantic Geotraces cruises. *J. Mar. Syst.* 126:3–23
- Vance D, Little SH, de Souza GF, Khatiwala S, Lohan MC, Middag R. 2017. Silicon and zinc biogeochemical cycles coupled through the Southern Ocean. *Nat. Geosci.* 10:202–6
- Velasquez IB, Ibanami E, Maas EW, Boyd PW, Nodder S, Sander SG. 2016. Ferrioxamine siderophores detected amongst iron binding ligands produced during the remineralization of marine particles. *Front. Mar. Sci.* 3:172
- Völker C, Tagliabue A. 2015. Modeling organic iron-binding ligands in a three-dimensional biogeochemical ocean model. *Mar. Chem.* 173:67–77
- von der Heyden BP, Roychoudhury AN. 2015. A review of colloidal iron partitioning and distribution in the open ocean. *Mar. Chem.* 177:9–19
- von der Heyden BP, Roychoudhury AN, Mtshali TN, Tyliczszak T, Myneni SCB. 2012. Chemically and geographically distinct solid-phase iron pools in the Southern Ocean. *Science* 338:1199–201
- Weber T, John S, Tagliabue A, DeVries T. 2018. Biological uptake and reversible scavenging of zinc in the global ocean. *Science* 361:72–76
- Whitby H, Posacka AM, Maldonado MT, van den Berg CMG. 2018. Copper-binding ligands in the NE Pacific. *Mar. Chem.* 204:36–48
- Wozniak AS, Shelley RU, McElhenie SD, Landing WM, Hatcher PG. 2015. Aerosol water soluble organic matter characteristics over the North Atlantic Ocean: implications for iron-binding ligands and iron solubility. *Mar. Chem.* 173:162–72
- Wozniak AS, Shelley RU, Sleighter RL, Abdulla HAN, Morton PL, et al. 2013. Relationships among aerosol water soluble organic matter, iron and aluminum in European, North African, and marine air masses from the 2010 US GEOTRACES cruise. *Mar. Chem.* 154:24–33
- Wozniak AS, Willoughby AS, Gurganus SC, Hatcher PG. 2014. Distinguishing molecular characteristics of aerosol water soluble organic matter from the 2011 trans-North Atlantic US GEOTRACES cruise. *Atmos. Chem. Phys.* 14:8419–34
- Wyatt NJ, Milne A, Woodward EMS, Rees AP, Browning TJ, et al. 2014. Biogeochemical cycling of dissolved zinc along the GEOTRACES South Atlantic transect GA10 at 40°S. *Glob. Biogeochem. Cycles* 28:44–56

- Xie RC, Galer SJG, Abouchami W, Rijkenberg MJA, De Jong J, et al. 2015. The cadmium–phosphate relationship in the western South Atlantic—the importance of mode and intermediate waters on the global systematics. *Mar. Chem.* 177:110–23
- Zheng X-Y, Plancherel Y, Saito MA, Scott PM, Henderson GM. 2016. Rare earth elements (REEs) in the tropical South Atlantic and quantitative deconvolution of their non-conservative behavior. *Geochim. Cosmochim. Acta* 177:217–37
- Zurbrick CM, Boyle EA, Kayser RJ, Reuer MK, Wu J, et al. 2018. Dissolved Pb and Pb isotopes in the North Atlantic from the GEOVIDE transect (GEOTRACES GA-01) and their decadal evolution. *Biogeosciences* 15:4995–5014